

2018-06-12

PALEOECOLOGICAL ANALYSIS OF BENTHIC RECOVERY AFTER THE LATE PERMIAN MASS EXTINCTION EVENT IN EASTERN LOMBARDY, ITALY

Foster, W

<http://hdl.handle.net/10026.1/11171>

10.2110/palo.2017.079

PALAIOS

Society for Sedimentary Geology

All content in PEARL is protected by copyright law. Author manuscripts are made available in accordance with publisher policies. Please cite only the published version using the details provided on the item record or document. In the absence of an open licence (e.g. Creative Commons), permissions for further reuse of content should be sought from the publisher or author.

1 **PALEOECOLOGICAL ANALYSIS OF BENTHIC RECOVERY**
2 **AFTER THE LATE PERMIAN MASS EXTINCTION EVENT**
3 **IN EASTERN LOMBARDY, ITALY.**

4 WILLIAM J. FOSTER^{1*}, SILVIA DANISE², GREGORY D. PRICE² and RICHARD, J.
5 TWITCHETT³

6 ¹*Jackson School of Geosciences, University of Texas at Austin, Austin, Texas 78722 USA.*

7 *w.j.foster@gmx.co.uk* ²*School of Geography, Earth & Environmental Sciences, University of*

8 *Plymouth, Plymouth, PL4 8AA, UK.* ³*Dept. of Earth Sciences, Natural History Museum,*

9 *London, SW7 5BD, UK.*

10 **Corresponding author. Current address: Museum für Naturkunde, Leibniz-Institut*
11 *für Evolutions- und Biodiversitätsforschung, Berlin, Germany.*

12 Key words: Paleotethys; marine invertebrates; Early Triassic; Habitable zone; Werfen
13 Formation.

14 **ABSTRACT:**

15 The late Permian mass extinction was the most severe biotic crisis of the Phanerozoic, with
16 associated environmental changes that included the expansion of hypoxic and anoxic
17 conditions in shallow shelf settings. It has been hypothesized that wave aeration promoted
18 oxygen transport to the seafloor providing a ‘habitable zone’ in the shallowest marine
19 environments that allowed the survival and rapid recovery of benthic invertebrates during the
20 Early Triassic. We test this hypothesis by studying the rock and fossil records of the Lower
21 Triassic Servino Formation, Italy. We also provide the first $\delta^{13}\text{C}_{\text{carb}}$ isotope curve, and present
22 new occurrence data of stratigraphically important fossils (i.e. cf. *Tirolites cassianus*), to
23 improve the stratigraphic framework of the Servino Formation. The low-diversity fossil
24 assemblages of the Servino Formation have similar compositions to other western Paleotethyan
25 localities. Facies analysis demonstrates that benthic invertebrates were restricted to wave-
26 aerated settings, supporting the proposed ‘habitable zone’ hypothesis. However, there is no
27 evidence for rapid recovery in the ‘habitable zone’ prior to the Spathian, which may indicate
28 additional environmental stresses. In the lower Spathian Myophoria Beds Member, an increase

29 in taxonomic and functional richness, the appearance of stenohaline, erect taxa, significant
30 turnover, and increased heterogeneity in the composition of benthic assemblages indicate
31 significant benthic recovery, which is attributed to reduced environmental stress. Prior to the
32 late Spathian “Upper Member”, bioturbation is poorly developed and restricted to only a few
33 thin horizons, but in the “Upper Member” the intensity of bioturbation and proportion of
34 bioturbated rock increase. This change can be attributed to climatic cooling and a related
35 decrease in environmental stress. This upper Spathian recovery pulse can now be traced across
36 the western Paleotethys, in both nearshore and deep offshore (below wave base) settings.

37

39 The late Permian mass extinction event was the most severe biotic crisis in Earth's
40 history (McGhee et al., 2004). Although the causal mechanisms remain the subject of
41 considerable debate, most studies recognize that the extinction is associated with climate-
42 induced environmental changes triggered by Siberian Trap volcanism (Algeo et al., 2011;
43 Burgess and Bowring, 2015). Anoxia, euxinia, high sea-surface temperatures, and ocean
44 acidification have been invoked as the leading drivers of extinctions in the oceans (e.g. Wignall
45 and Twitchett 1996; Grice et al. 2005; Knoll et al. 2007; Kearsley et al. 2009; Nabbefeld et al.
46 2010; He et al. 2015; Wignall et al. 2016). However, other environmental changes, including
47 increased sediment fluxes, eutrophication, and sea-level rise are thought to have contributed to
48 the severity of the event (Algeo and Twitchett, 2010; Algeo et al., 2011; Schobben et al., 2015).
49 Despite its taxonomic severity, the late Permian mass extinction event did not cause a major
50 decline in global functional diversity, with only one mode of life identified as going globally
51 extinct (Foster and Twitchett, 2014).

52 In order to understand the mechanisms involved in the late Permian mass extinction
53 and the subsequent recovery, paleoecologists have investigated changes in the species richness
54 and ecological complexity (e.g. presence/absence of key taxa, both the spatial and temporal
55 distribution of taxa, changes in body size, evenness, and functional diversity) of marine
56 communities. An increasing body of evidence based on the distribution of benthic invertebrates
57 along a water depth gradient across the extinction event and during the Early Triassic has
58 shown that relatively diverse and ecologically complex benthic marine fossil assemblages were
59 restricted to shallow oxygenated settings aerated by wave activity, i.e. the 'habitable zone', e.g.
60 Sverdrup Basin, Liard Basin, Peace River Embayment, and Kananaskis, Canada (Beatty et al.
61 2008; Zonneveld et al. 2010); Perth Basin, Australia (Chen et al. 2012), western U.S (Mata and
62 Bottjer, 2011; Pietsch et al. 2014); Aggtelek Karst, Hungary (Foster et al. 2015); Svalbard

63 (Foster et al., 2017a); Dolomites, Italy (Foster et al., 2017); and South China (He et al. 2015).
64 However, when considering the species richness and ecological complexity of benthic
65 communities not all locations show rapid recovery, e.g. Aggtelek Karst (Foster et al., 2015;
66 Foster and Sebe, 2017), western U.S (Hofmann et al., 2013), and South China (Payne et al.,
67 2006b; Chen et al., 2007; 2012), demonstrating that there is a temporal and regional dynamic
68 to the recovery with advanced recovery within the ‘habitable zone’ not occurring until the
69 Spathian in these locations. Furthermore, even though there are marine communities that
70 signify advanced recovery during the Early Triassic their ecological complexity does not
71 indicate ‘full recovery’, which is not observed until the Middle Triassic (e.g. Erwin and Pan,
72 1996; Twitchett, 2006; Payne et al., 2011; Foster and Sebe, 2017). The refuge, therefore, was
73 severely stressed by other factors, with paleontological, geochemical, and sedimentological
74 proxies suggesting that sediment fluxes, eutrophication, salinity fluctuations and high
75 temperatures, limited the recovery of marine ecosystems (Posenato, 2008; Algeo and Twitchett,
76 2010; Sun et al., 2012; Pietsch et al., 2014; 2016; Foster et al. 2015, 2017; Schobben et al.,
77 2013; 2015).

78 Quantitative paleoecological studies of Early Triassic benthic macroinvertebrates are
79 limited to only a few regions, in particular the western U.S. (Schubert and Bottjer, 1995;
80 McGowan et al., 2009; Hofmann et al., 2013; 2014; Pietsch et al., 2014), central Europe
81 (Hofmann et al., 2015; Foster et al., 2015; 2017a; Pietsch et al., 2016), and South China (Payne
82 et al., 2006; Hautmann et al., 2015; Zhang et al., 2017; Foster et al., 2018), and to only a few
83 localities within those regions. Demonstrating that quantitative paleoecology is an
84 underutilized tool in understanding the recovery of marine communities following the late
85 Permian mass extinction event. Despite the rich paleontological history in central Europe only
86 two areas have been quantitatively studied, i.e. the Dolomites, Italy (Hofmann et al., 2015;
87 Pietsch et al., 2016; Foster et al., 2017a) and the Aggtelek Karst, Hungary (Foster et al., 2015).

88 Understanding of benthic marine recovery in the western Paleotethys is, therefore, incomplete.
89 The main aim of this study is to quantify the recovery of benthic invertebrates following the
90 late Permian mass extinction by analyzing changes in the species richness, functional richness,
91 evenness, composition, and ecological complexity of benthic marine communities from the
92 Lower Triassic Servino Formation of eastern Lombardy, Italy. This formation represents a
93 more marginal setting than that recorded by the Werfen Formation in the Dolomites, and has
94 hitherto not been quantitatively studied. In particular, we aim to (i) test if ecologically complex
95 benthic communities that represent advanced recovery were restricted to settings aerated by
96 wave activity, and (ii) assess if there is a temporal aspect within the hypothesized habitable
97 zone. These data will then be compared to results from other localities within this region and
98 placed in a global context.

99

100

GEOLOGICAL SETTING AND STUDY SITES

101

102

103

104

105

106

107

108

109

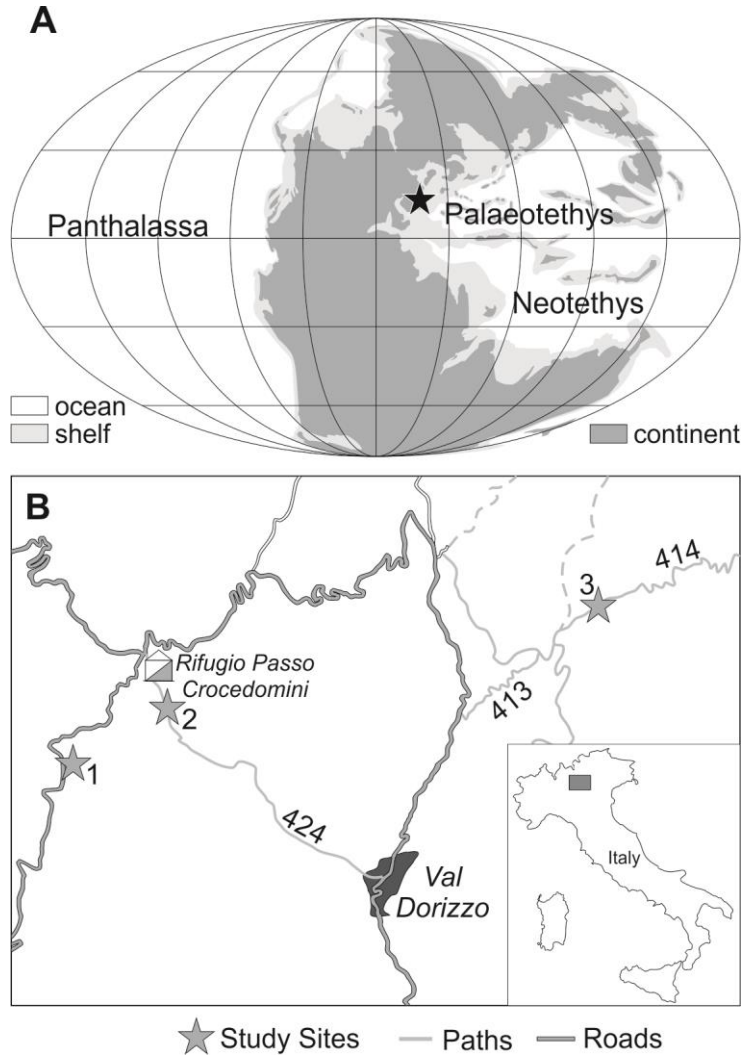
110

111

112

The Lower Triassic of northern Italy records deposition on the northwestern margin of the Paleotethys Ocean (Fig. 1A). The Lower Triassic successions of northern Italy have been assigned to two different formations: the Werfen Formation to the east and the Servino Formation to the west (Assereto et al., 1973). The Servino Formation extends from Campione d'Italia to Valli Giuducarie and in the foothills of the Tre Valli Bresciane, and due to Neoalpine underthrusting it is exposed on limbs of four anticlines: the Orobic, Trabuchello-Cabianca, Cedegolo, and Camuna (De Donatis and Falletti, 1999; Sciunnach et al., 1999). The Servino Formation differs from the Werfen Formation in that it represents a more marginal depositional setting with higher terrigenous content (Cassinis, 1968; Assereto et al., 1973; Neri, 1986). Despite this difference, some facies can be recognized in both formations. The Servino Formation is also more condensed than the Werfen Formation, being approximately 100-150m thick, and paraconformably overlies the Permian Verrucano Lombardo Formation (Assereto et

113 al., 1973; De Donatis and Falletti, 1999). Due to the extensional conditions that existed in the
114 western Paleotethys during the Triassic (e.g. Doglioni 1987) not all of the members or units
115 recognized in the Werfen Formation can be traced to the Servino Formation (Fig. 2).



116

117 **FIGURE 1: Geological setting and locality map of the Servino Formation, Italy.** A)
118 Paleogeographic map of the Early Triassic after Blakey (2012) indicating the approximate
119 position of the Servino Formation (black star). B) Locality maps of the study sites in eastern
120 Lombardy: 1.Mt.Rondenino road cut. 2. Path 424. 3. Path 414.

121

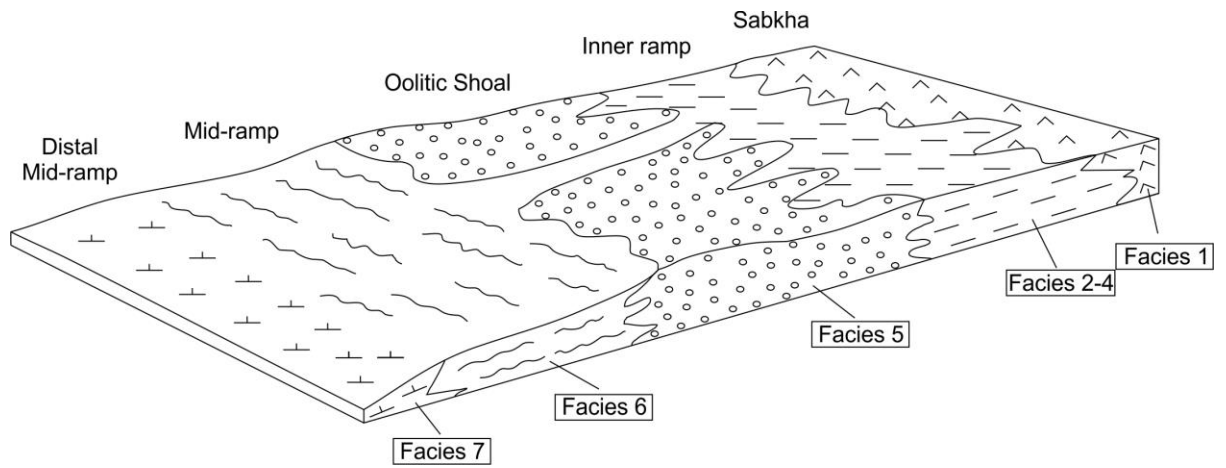
		Lombardy	Dolomites	Balaton Highland	Aggtelek Karst		
Anisian		Carniola di Bovegno ?	Lower Serla Dolomite	Aszofó Dolomite	Gutenstein		
Early Triassic	Olenekian	Servino	San Lucano	Hidegkut Csopak Marl	Upper Unit	Szinpetri Limestone	
			"Upper Member"		Cencenighe	Middle Unit	Szin Marl
			? Myophoria Beds		Val Badia	Lower Unit	
			Acquaseria		Campil	HDM	Bódvaszilas Sandstone
	Gastropod Oolite	Gastropod Oolite	Hidegkut Homoko				
	Ca' San Marco	Werfen	Koveskal Dolomite	Balatonfelvidék Sandstone			
	Praso Limestone				Siusi		
	Prato Solaro				Andraz		
					Mazzin		
					Tesero		
Permian	Verrucano Lombardo	Bellerophon			Perkupa Evaporite		

122

123 **FIGURE 2: Lithostratigraphic framework for eastern Lombardy and central European**
124 **sections discussed in the text.** Formation names are in bold; Lombardy, Italy (modified from
125 Sciunnach et al., 1999); Dolomites, Italy (after Posenato, 2008b); Balaton Highland, Hungary
126 (after Broglio Loriga et al., 1990), HDM=Hidegkut Dolomite Member; Aggtelek Karst,
127 Hungary (after Foster et al., 2015).

128

129 Deposition of the Servino Formation occurred on a shallow epicontinental shelf mostly
130 on the landward side of oolitic shoals in a restricted setting (Assereto and Rizzini, 1975; Neri,
131 1986). The lithology and facies of the mixed siliciclastic-carbonate succession are similar to
132 those recognized in the Balaton Highlands, Hungary (a.k.a Transdanubian Range; WJF pers.
133 obs.). Seven facies were recognized in this study (Table 1; Fig. 3) following detailed
134 descriptions of the facies and ramp evolution of coeval western Paleotethyan localities,
135 representing: marine sabkha, peritidal, inner ramp, shoal, mid-ramp, and distal mid-ramp
136 depositional environments (Assereto and Rizzini, 1975; Broglio Loriga et al., 1990; Hips, 1998;
137 Török, 1998; De Donatis and Falletti, 1999; Sciunnach et al., 1999).



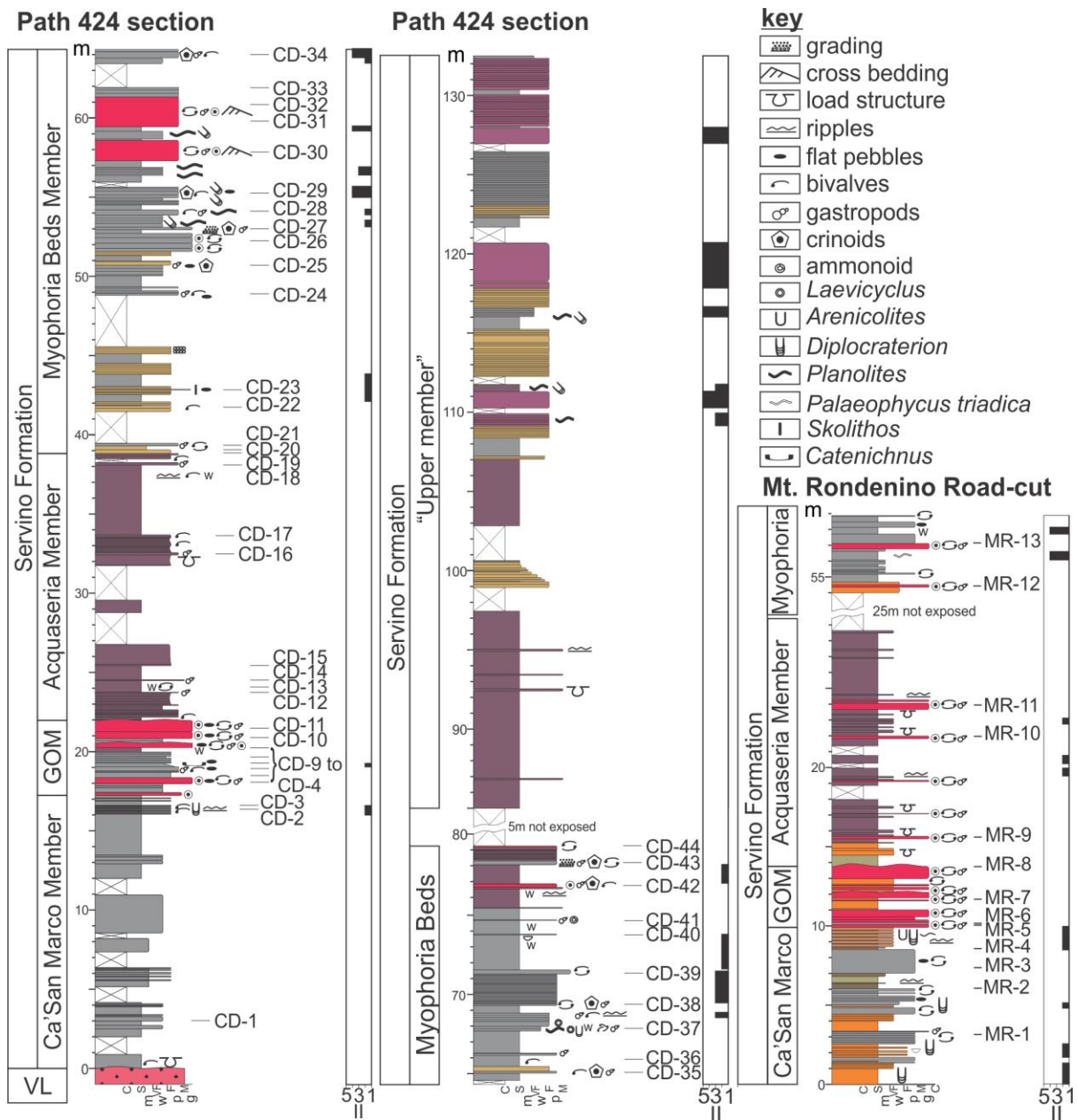
138

139 **FIGURE 3. Schematic model of the depositional environments of the Servino**
140 **Formation, East Lombardy.** Facies descriptions are in Table 1. Modified from Hips and
141 Haas (2007).

TABLE 1: Sedimentary facies and depositional environments for the investigated Servino Formation.

Facies	Lithology	Sedimentary Structures	Depositional environment
1	Grey calcareous siltstones alternating with yellow dolomitic sandstones. Chicken-wire structured gypsum.	Parallel-laminated siltstones alternating with bedded vuggy sandstones. Flat pebbles. Bivalves occur convex-up at the base of sandstone beds. <i>Skolithos</i> and gastropods also occur.	Marine sabkha (supratidal to peritidal)
2	Fine- to medium-grained purple sandstones.	Moderate to strong bioturbation (ii3-5) overprinting physical sedimentary structures. <i>Planolites</i> and <i>Rhizocorallium</i> . In the absence of bioturbation, beds are planar-laminated.	Inner ramp (subtidal sand flat)
3	Purple siltstones and sandstones	Planar laminated. Wrinkle marks and symmetrical ripple marks on bedding surfaces.	Inner ramp (subtidal, intershoal)
4	Grey silty mudstones interbedded with very fine sandstones and siltstones.	The sandstones have symmetrically rippled tops. The siltstones are laminated and occasionally with ball and pillow structures. Convex-up bivalves, <i>Diplocraterion</i> , <i>Rhizocorallium</i> and <i>Planolites</i> occur on bedding planes.	Inner ramp (subtidal, inter shoal)
5	Red-pink sandy oolitic limestones	Cross bedding in thicker beds (72-189cm) and planar bedding in thinner beds. Hummocky tops, flat pebbles, rhomboidal dolomite.	Ooid Shoal
6	Grey marly limestones	Laminated siltstones, wrinkle marks, symmetrical ripple marks, bivalves, gastropods, and crinoids. Bioturbation (ii1-4). <i>Planolites</i> , <i>Laevicyclus</i> , and <i>Diplocraterion</i> .	Mid-ramp
7	Grey siltstones interbedded with thin grey packstones.	Planar laminated and occasional gutter casts. Ammonoids, gastropods, bivalves, and wrinkle marks.	Distal mid-ramp

143 Three stratigraphic sections were investigated in this study from the Camuna anticline in
144 eastern Lombardy: Path 424 (N45° 54' 15.5" E010° 24' 43.8"), Maniva-Croce Domini road-
145 cut through Mount Rondenino (N45° 53' 42.8" E010° 23' 47.6"), and the Path 414 section
146 (N45° 54' 09.2" E010° 30' 11.5"; Fig. 1B). The Servino Formation is made up of six
147 members: Prato Solaro (including the Praso Limestone), Ca'San Marco, Gastropod Oolite,
148 Acquaseria, Myophoria Beds, and the "Upper Member" (Sciunnach et al., 1999). The Prato
149 Solaro Member was not observed in this study. The Path 424 section is a continuous section,
150 with few gaps, from the Permian Verrucano Lombardo Formation to the Middle Triassic
151 Carniola di Bovegno Formation (Fig. 4). The Mt. Rondenino road-cut section is exposed in
152 three outcrops: the southernmost exposes the Ca'San Marco to Myophoria Beds Member,
153 moving northwards, the next exposes the Acquaseria Member and the third exposes the
154 Myophoria Beds Member. The Path 414 section runs parallel to the River Bruffione, NE
155 beyond Passo Valdi, where small, <1 m, patchy exposures of the Myophoria Beds Member
156 are exposed.



157

158 **FIGURE 4: Measured sections of the Servino Formation along Path 424 and the Mount**
 159 **Rondenino road-cut showing stratigraphic intervals and sampling levels. Ichnofabric**
 160 **Index after Droser and Bottjer (1986). Grain size scale: C=clay, S=siltstone, VF=very fine**
 161 **sand, F=fine sand, M=medium sand, m=mudstone, w = wackestone, p = packstone, g=**
 162 **grainstone. Color in the lithology column refers to the rock color observed in the field.**

163

164

METHODS

165

Sedimentary logs were produced in the field in September 2012 and June 2013.

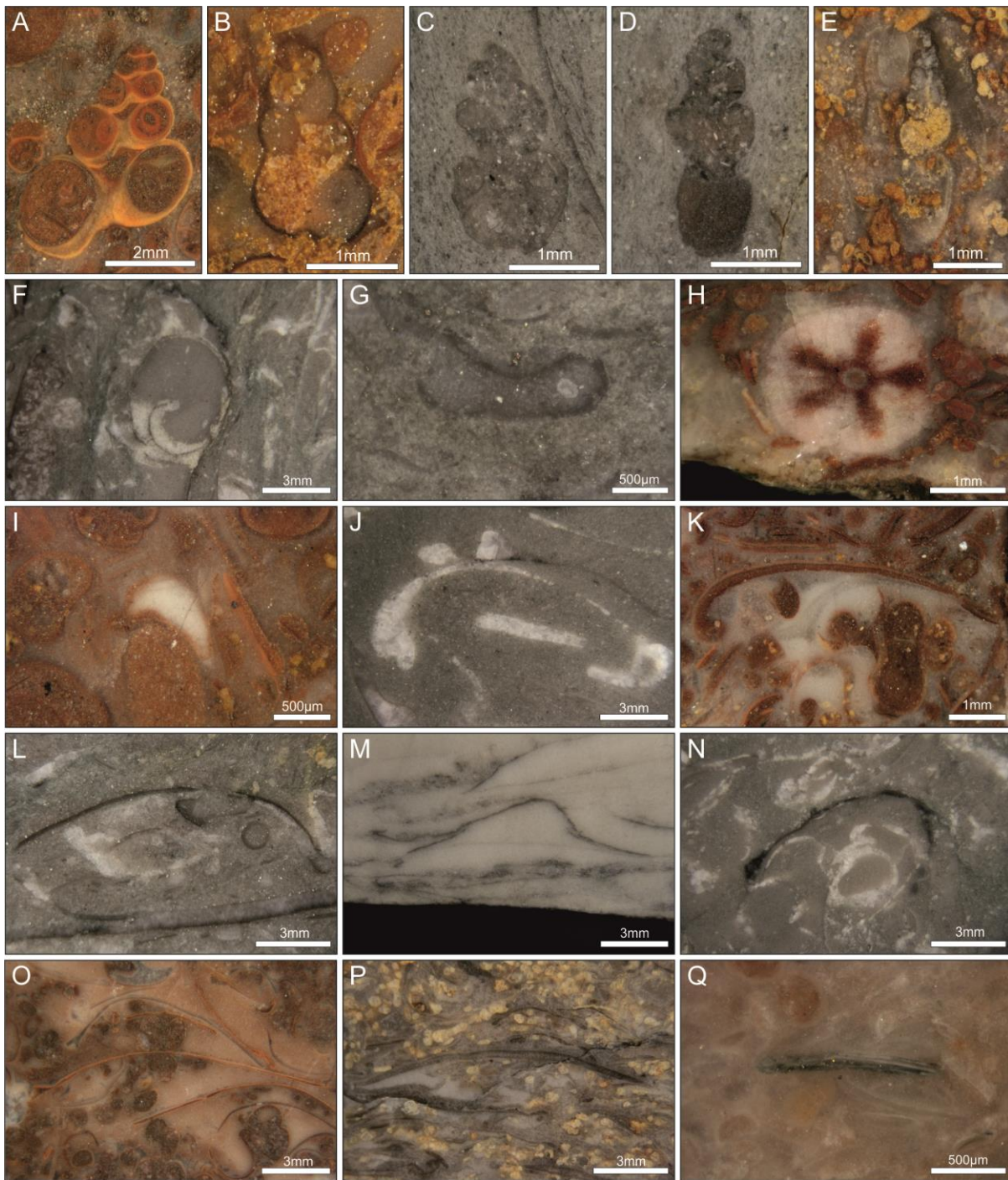
166

Lithologies, sedimentary structures, trace fossils and ichnofabric index (ii, Droser & Bottjer

167

1993) were described for each measured bed (Figs. 3-4). On fossiliferous bedding planes, all

168 fossils within a randomly placed 20 x 20 cm quadrat were counted and identified. This small
169 quadrat size was used due to the limited exposure of large bedding planes in the field, and
170 because enough fossils could be identified within this area for quantitative analysis
171 (typically >100 specimens). In addition, all other fossiliferous beds identified in the field were
172 quantitatively sampled for macrofossils using the polished slab technique (following Foster et
173 al. 2015). No fossiliferous horizons were, however, observed in the “Upper Member”. All
174 identifiable fossils in the polished slabs were identified to the most precise taxonomic level to
175 which they could be confidently assigned (Fig. 5; Supplementary Material). Descriptions from
176 previous studies of Lower Triassic fossils in polished slabs and thin sections were used to
177 determine the taxonomic assignments (Nützel and Schulbert, 2005; Foster et al., 2015, 2017a).
178 Taxonomic resolution varied between fossil groups, ranging from species- to phylum-level.



179

180 **FIGURE 5: Fossil invertebrates from polished slabs of the Servino Formation. A)**
 181 *Coelostylina werfensis*, Acquaseria Member, CD-12. **B)** *Polygrina* sp., Ca'San Marco
 182 Member, MR-01. **C-D)** Gastropod sp. A, Gastropod Oolite Member, CD-07. **E)** cf. *Allcosmia*
 183 sp., Myophoria Beds Member, CD-25. **F)** *Natiria costata*, Myophoria Beds Member, CD-43.
 184 **G)** *Microconchus* sp., Gastropod Oolite Member, CD-08. **H)** *Holocrinus*, Myophoria Beds
 185 Member, CD-42. **I)** Ophiuroidea, Acquaseria Member, CD-16. **J)** *Neoschizodus* spp.,
 186 Myophoria Beds Member, CD-39. **K)** Bivalve sp. A, Gastropod Oolite Member, CD-10. **L)**
 187 *Austrotindaria* spp., Myophoria Beds Member, CD-43. **M)** cf. *Bakevellia* spp., Ca'San Marco
 188 Member, CD-01. **N)** *Costatoria costata*, Myophoria Beds Member, CD-39. **O)** cf. *Eumorphotis*

189 spp., Gastropod Oolite Member, CD-11. **P)** cf. *Scythentolium* sp., Myophoria Beds Member,
190 MR-03. **Q)** *Lingularia* spp., Gastropod Oolite Member, CD-05.

191

192 To improve the stratigraphic framework of the Servino Formation, samples for
193 chemostratigraphy were collected every 20 cm from the Path 424 section. In the laboratory,
194 carbonate powders were drilled from fresh rock surfaces using a diamond-tipped drill. Cracks,
195 veins and fossil shells were avoided. Isotopes were determined on a VG Instruments Optima
196 Isotope Ratio Mass Spectrometer with a Gilson multiflow carbonate system (at Plymouth
197 University) using 500–1000 µg carbonate. Isotopic results were calibrated against NBS-19.
198 The $\delta^{13}\text{C}$ compositions are reported in per mil (‰) notation with respect to the V-PDB
199 international standard. Reproducibility for $\delta^{13}\text{C}$ was generally better than $\pm 0.1\text{‰}$.

200

201

Paleoecological Analysis

202 Paleoecological analyses were limited to benthic marine invertebrates and used the
203 minimum number of individuals (MNI) method following Foster et al. (2015). Samples with
204 <20 MNI were removed from the analysis. As multiple methods were used to collect the data
205 and most of the samples were polished slabs, the analysis was carried out using the finest
206 taxonomic resolution obtained with the polished slab technique, to allow different collection
207 methods to be analyzed synchronously. Functional diversity is becoming increasingly
208 recognized as an important driver of ecosystem functioning, and each taxon was, therefore,
209 assigned to a bin in the ecospace model of Bambach et al. (2007) based on its tiering, motility,
210 and feeding (following Foster and Twitchett, 2014), using data from extant relatives, previous
211 publications, and functional morphology. In cases where interpretation of a taxon's
212 classification is problematic, the most up-to-date or most widely accepted analysis was
213 followed. Unidentified taxa or taxa assigned to higher levels were assigned to a bin in the
214 ecospace model based on comparisons of their morphology with other known taxa. Other

215 ecospace models (e.g. Novack-Gottshall, 2007) include other parameters, such as reproduction
216 mode and preferred substrate, which can provide a finer resolution of ecological change than
217 the Bambach et al. (2007) ecospace model used in this study. These other models, however,
218 could not be applied in this study as they were either uniform across the identified taxa, or the
219 classification for the identified species is unknown.

220 Diversity was measured using species richness (S), and functional richness (the number
221 of modes of life in a sample), and the Simpson Diversity Index ($1-D$) was calculated for both
222 species and functional richness. As the number of individuals varied between samples, the
223 Simpson Diversity Index was converted to an effective diversity (Δ ; Jost 2007), which allows
224 the impact of evenness on richness to be quantified, i.e. effective diversity and functional
225 effective diversity, respectively. The Kruskal-Wallis test was used to investigate differences in
226 the median diversity between different units/members, facies and substages.

227 For multivariate elaboration, relative, rather than absolute, abundances were used as
228 preservation varies between samples and multiple sampling methods were used. The data were
229 square-root transformed to de-emphasize the influence of the most dominant taxa (Clarke and
230 Warwick, 2001). Cluster analysis using an unweighted pair-group average cluster model
231 (Clarke and Warwick, 2001), and the Bray-Curtis similarity matrix, was applied to recognize
232 those species that tend to co-occur in samples and to group together samples of similar
233 taxonomic composition. The similarity profile test (SIMPROF) was applied to determine
234 significant differences between the clusters (Clarke and Warwick, 2001). Here, 999
235 permutations were applied to calculate a mean similarity profile, 999 simulated profiles were
236 generated, and the chosen significance level was 0.05. The resulting clusters of samples were
237 analyzed through a similarity percentages routine (SIMPER) to determine which taxa were
238 responsible for the greatest similarity within groups. This method enabled the identification of
239 groups of samples that contain a similar suite of taxa in similar proportions (i.e. biofacies), and

240 also to identify their characteristic taxa. Non-metric multidimensional scaling (nMDS) was
241 then applied to visualize trends and groupings of the samples.

242 A permutational ANOVA (PERMANOVA) was used to compare the benthic
243 assemblages between the different members and facies of the Servino Formation (Anderson
244 2001). Because there are not always enough possible unique permutations to get a reasonable
245 test (Anderson, 2001), *p*-values were also calculated with the Monte Carlo method. When
246 multiple variables, e.g. member, facies, or lithology, showed significant differences, they were
247 then subject to pair-wise comparisons. This was done by performing a (two-tailed) t-test, with
248 significance taken at the 0.05 level.

249 Cluster, ordination, and PERMANOVA analyses were performed with the software
250 PRIMER 6.1.15 & PERMANOVA 1.0.5.

251

252 STRATIGRAPHY AND CORRELATION

253 Biostratigraphy

254 The Prato Solaro and Praso Limestone members were not observed in this study, but
255 have been recorded in the nearby Passo Valdi section (Cassinis 1968). The bivalves *Claraia*
256 *intermedia* and *C. aurita* occur 7 m and 15 m above the base of the Ca'San Marco Member in
257 the Valsassina (Posenato et al., 1996) and Val Fontanelle Valley sections (Cassinis, 1990;
258 Cassinis et al., 2007), respectively, which suggests correlation with the Dienerian *C. aurita*
259 Bivalve Zone of the Italian Werfen Formation (e.g. Posenato 2008). Ichnological studies of the
260 western Paleotethys record a stepwise reappearance of ichnotaxa that is unrelated to facies
261 change following the late Permian mass extinction in (Twitchett, 1999; Twitchett and Barras,
262 2004; Hofmann et al., 2011; Foster et al., 2015), and the reappearance of certain ichnotaxa can
263 be used as a stratigraphic tool in the absence of stratigraphically useful body fossils (Twitchett
264 and Barras, 2004). Thin micaceous sandstones of the Ca'San Marco Member contain a trace

265 fossil assemblage dominated by small (2 - 6mm) diameter *Diplocraterion*. Twitchett and Barras
266 (2004) correlated this *Diplocraterion*-dominated ichnofacies of the Ca' San Marco Member
267 with a similar one that characterizes the upper Siusi Member of the Werfen Formation.

268 Conodont elements belonging to *Ellisonia triassica*, *Hadrodontina anceps*,
269 *Pachycladina obliqua* and *Foliella gardenae* have also been recovered from the overlying
270 Gastropod Oolite and Acquaseria Members of the Servino Formation (Twitchett, 2000). This
271 assemblage indicates correlation with the Smithian *Parachirognathus-Furnishius* Conodont
272 Zone (Sweet et al., 1971; Twitchett, 2000; Aljinović et al., 2006, 2011).

273 The Myophoria Beds Member records the first appearance of the ichnospecies
274 *Palaeophycus triadica* and the ichnogenus *Rhizocorallium*. Twitchett (1997) used the
275 occurrence of *P. triadica* to correlate this member of the Servino Formation with the lower
276 Spathian Val Badia Member of the Werfen Formation. Similarly, Twitchett and Barras (2004)
277 also used the occurrence of *Rhizocorallium* to correlate this member with the Val Badia
278 Member. Elsewhere, the Spathian ammonoid *Dinarites* sp. has been recorded from this member
279 in the Val Fontanalle Valley and Passo Valdi sections (Neri, 1986; Cassinis, 1990). In this
280 study, cf. *Tirolites cassianus* was recorded 36 m above the base of the Myophoria Beds
281 Member in the Path 424 section, and is correlated with the Spathian *Tirolites cassianus* Zone
282 (*sensu* Posenato 1992). Spathian bivalves and gastropods, e.g. *Natiria costata*, *Costatoria*
283 *costata*, and cf. *Eumorphotis telleri*, are also recorded throughout this member. The Myophoria
284 Beds Member is, therefore, correlated with the lower Spathian Val Badia Member, Italy and
285 the lower part of the Csopak Marl Formation, Hungary. In the "Upper Member" only
286 *Meandrospira pusilla* has been recorded (Gaetani, 1982) which may correspond with the
287 Spathian Cencenighe and San Lucano Members of the Werfen Formation (Broglia Loriga et
288 al., 1990); this species has, however, also been recorded from the Middle Triassic (Sciunnach
289 et al., 1999).

290

291

Carbonate Carbon Isotopes

292

293

294

295

296

297

298

299

300

301

302

303

304

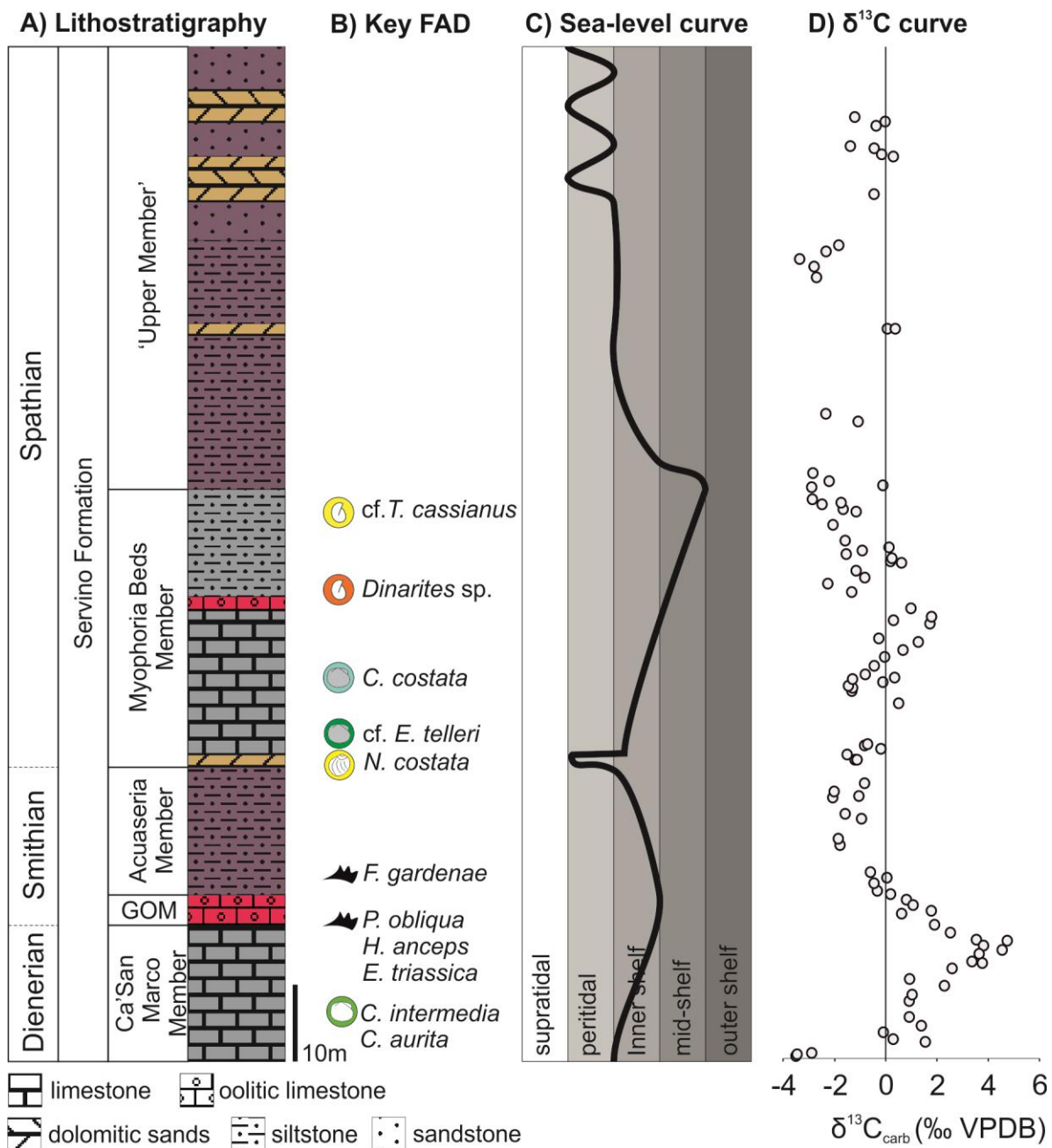
305

306

307

308

The Permian/Triassic boundary and subsequent Early Triassic is characterized by a number of large negative and positive carbon isotope excursions (Payne et al., 2004) that makes it possible to correlate different sections from around the globe in the absence of biostratigraphic markers, e.g. the Induan/Olenekian Boundary (Horacek et al., 2007; Posenato, 2008a; Grasby et al., 2013). Two major positive carbon isotope excursions are recorded in the Path 424 section (Fig. 6). The first positive peak of +4.7‰ occurs near the top of the Ca’San Marco Member, in the absence of a facies change. Isotope values then fall to -2.0‰ in the Acquaseria Member (Fig. 6). This first peak is correlated with an isotope peak that occurs around the Induan/Olenekian boundary and has been recognized from a number of different regions (Payne et al., 2004; Horacek et al., 2007, 2009; Grasby et al., 2013; Chen et al., 2016). A second positive excursion with a peak of +1.7‰ occurs 18 m above the base of the Myophoria Beds Member (Fig. 6), and correlates with an isotope peak in the lower Spathian Val Badia Member (Horacek et al., 2007; Foster et al., 2017a). The carbonate content of the “Upper Member” samples is low and only 16 samples yielded data, making any correlation equivocal. The rising values suggest deposition during the late Spathian (Payne et al., 2004), with the Lower/Middle Triassic boundary tentatively placed at the base of the overlying Carniola di Bovegno Formation (Sciunnach et al., 1999).



309

310 **FIGURE 6: Summary stratigraphy of the Lower Triassic Servino Formation, Italy.**
 311 Lithostratigraphy following Sciunnach et al. (1999), vertical subdivision is thickness
 312 proportional after Path 424 section. GOM = Gastropod Oolite Member. FAD = First
 313 appearance datums. Occurrences of *Claraia intermedia* after Posenato et al. (1996) and
 314 occurrences of *C. aurita* and *Dinarites* sp. after Cassinis et al. (2007). All other FAD's after
 315 this study. Sea-level curve from this study. Carbon isotope curve are from Path 424 section
 316 (this study).

317

318 PALEOECOLOGICAL RESULTS

319 Alpha Diversity

320 A total of 10,248 individuals were identified in 58 samples from the Servino Formation
321 and represent 21 taxa including bivalves, gastropods, ophiuroids, crinoids, brachiopods,
322 ostracods, microconchids, and ammonoids (Table 2; Fig. 5). The MNI per sample ranges from
323 1 to 1078, and 41 samples have a sufficiently large abundance (>20 MNI) for quantitative
324 analysis.

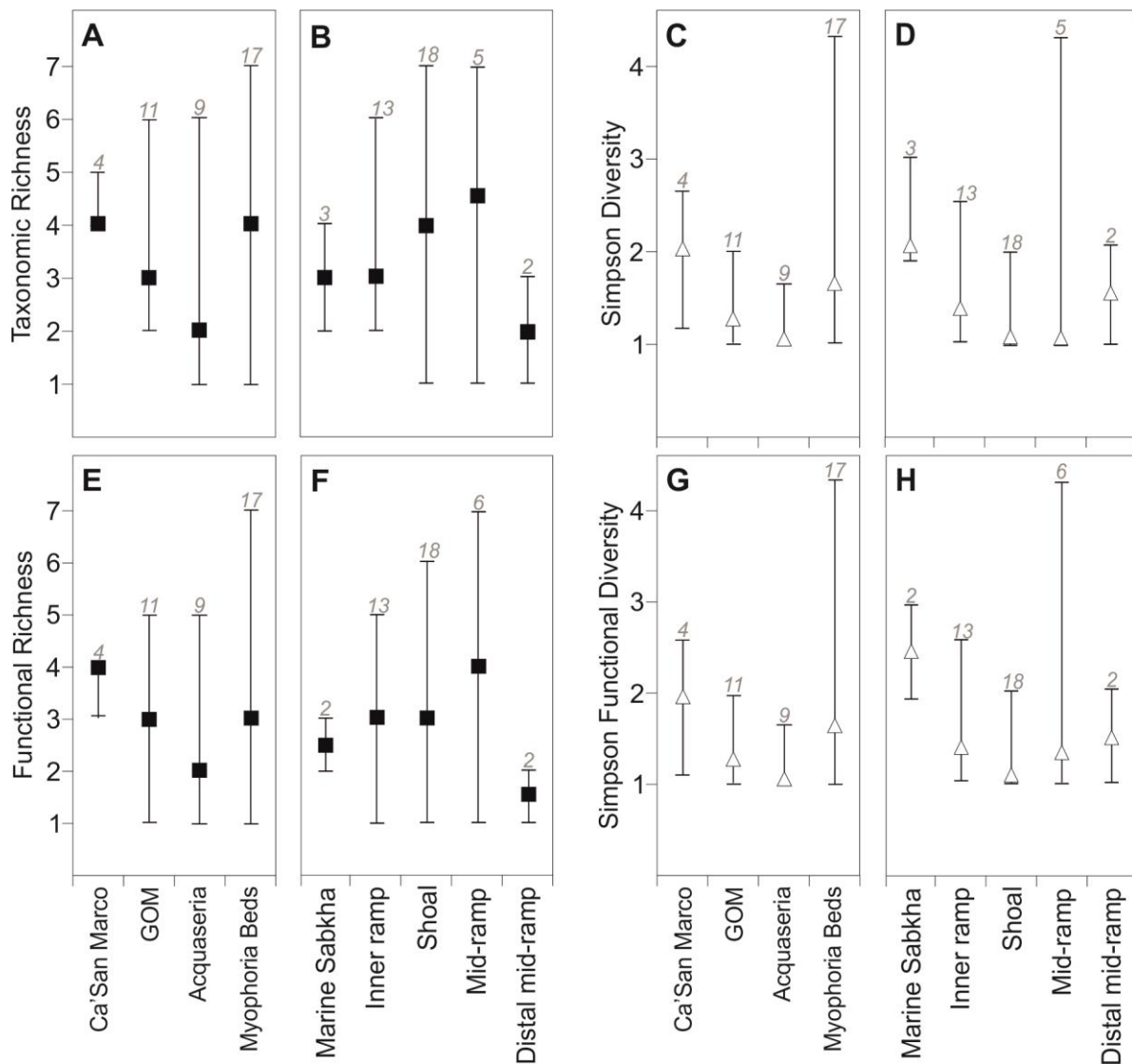
325 The richness of samples ranges from 1 to 7 and the effective diversity ranges from 1
326 to 4.3 (Figs. 7A-D). The most diverse samples, in terms of richness and diversity, come from
327 the Myophoria Beds Member in both the shoal and mid-ramp sedimentary facies (Fig. 7B,
328 7D). The least diverse samples also come from the same member and sedimentary facies, as
329 well as from the Acquaseria Member (Fig. 7B, 7D). Sample richness and effective diversity
330 among stratigraphic units show very similar patterns (Fig. 7A-D). Differences in species
331 richness between the different members are not significant ($p = 0.11$), but differences in
332 effective diversity are ($p = 0.02$), and pairwise comparisons show that effective diversity is
333 significantly lower in the Acquaseria Member than in the Ca' San Marco and Myophoria Beds
334 members (Fig. 7C).

335 **TABLE 2: List of all recorded taxa and their mode of life.** Modes of life after Bambach et
 336 al. (2007). T = Tiering: 2 = erect, 3 = epifaunal, 4 = semi-infaunal, 5 = shallow infaunal. M =
 337 Motility: 2 = slow, 4 = facultative, attached, 3 = facultative, unattached, 5 = unattached, 6 =
 338 attached. F = Feeding: 1 = suspension feeding, 2 = surface deposit feeding, 3 = miner, 4 =
 339 grazer, 5 = predator.

340

Species	Group	Mode of Life			Taxonomic Identification after
		T	M	F	
<i>Austrotindaria? canalensis</i>	Bivalve	5	3	1	Foster <i>et al.</i> (2016)
<i>Austrotindaria antiqua</i>	Bivalve	5	3	1	Foster <i>et al.</i> (2016)
cf. <i>Bakevella</i> spp.	Bivalve	4	6	1	Neri and Posenato (1985)
cf. <i>Bakevella albertii</i>	Bivalve	3	6	1	Neri and Posenato (1985)
<i>Costatoria costata</i>	Bivalve	5	3	1	Broglia Loriga and Posenato (1986)
cf. <i>Eumorphotis</i> spp.	Bivalve	3	6	1	Broglia Loriga and Mirabella (1986)
<i>Eumorphotis multiformis</i>	Bivalve	3	6	1	Broglia Loriga and Mirabella (1986)
cf. <i>Eumorphotis telleri</i>	Bivalve	3	6	1	Broglia Loriga and Mirabella (1986)
<i>Neoschizodus</i> sp.	Bivalve	5	3	1	Neri and Posenato (1985)
<i>Neoschizodus laevigatus</i>	Bivalve	5	3	1	Neri and Posenato (1985)
<i>Neoschizodus ovatus</i>	Bivalve	5	3	1	Neri and Posenato (1985)
cf. <i>Scythentolium</i> sp.	Bivalve	3	5	1	Neri and Posenato (1985)
Bivalve sp. A	Bivalve	5	3	1	
Bivalve sp. B	Bivalve	3	6	1	
cf. <i>Allocosmia</i> sp.	Gastropod	3	3	1	Posenato (1985)
<i>Coelostylina werfensis</i>	Gastropod	3	3	1	Nützel and Schulbert (2005)
<i>Polygyrina</i> sp.	Gastropod	3	3	1	Nützel and Schulbert (2005)
Gastropod sp. A	Gastropod	3	3	1	
<i>Natiria costata</i>	Gastropod	3	2	4	Neri and Posenato (1985)
<i>Lingularia</i> spp.	Brachiopod	5	4	1	Posenato <i>et al.</i> (2014)
<i>Holocrinus</i> sp.	Crinoid	2	4	1	Kashiyama and Oji (2004)
Ophiuroidea	Ophiuroid	3	2	1/2	Glazek and Radwański (1968)
Ostracod	Ostracod	3	2	2	
<i>Microconchus</i> sp.	Microconchid	3	6	1	Zatoń <i>et al.</i> (2013)

341



343

344 **FIGURE 7: Changes in sample richness in the Servino Formation, northern Italy.** A - B)
 345 Species richness of the Servino Formation, split by the different (A) formations, and (B)
 346 depositional environments. C - D) Simpson Diversity of the Servino Formation, split by the different (C)
 347 formations, and (D) depositional environments. E - F) Functional richness of the
 348 Servino Formation, split by the different (E) formations, and (F) depositional environments. G
 349 - H) Simpson Functional Diversity of the Servino Formation, split by the different (G)
 350 formations, and (H) depositional environments. Black squares and white triangles represent
 351 median values, and the maximum and minimum values are shown with short horizontal lines.
 352 Grey italics indicate the number of samples.

353

354 Changes in the alpha diversity of samples do not appear to be controlled by the
 355 environment. Median richness increases from the marine sabkha to mid-ramp settings before
 356 dropping in the distal mid-ramp (Fig. 7D). The differences, however, are not significant

357 ($p=0.53$), and the ranges of species richness values between the environments overlap (Fig 7B),
358 suggesting that there is no significant environmental control. The median effective diversity
359 values, on the other hand, are low, with highest values in the mid-ramp environment (Fig. 7D)
360 and show an inverse trend to sample richness. Even though this difference is not significant
361 ($p=0.09$), pairwise comparisons show that effective diversity is significantly lower in shoals
362 than in inner-ramp and marine sabkha settings (Fig. 7D).

363

364 Functional diversity

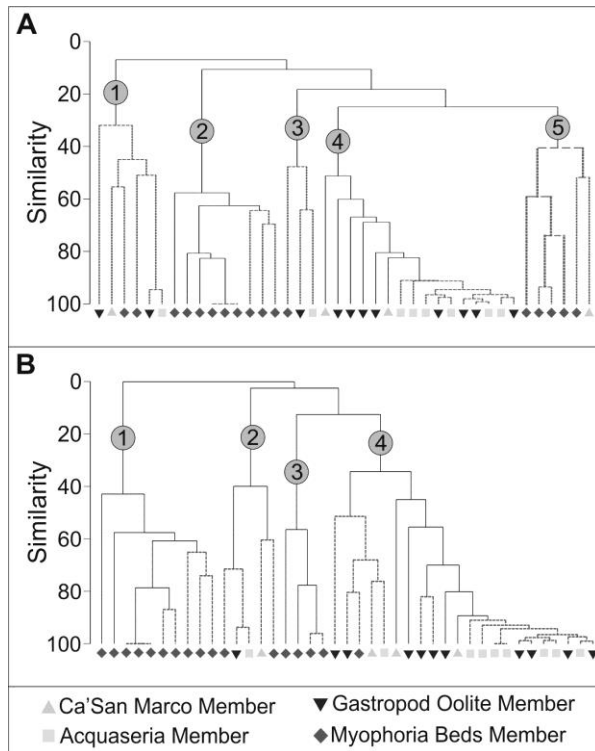
365 The recorded Servino Formation taxa represent eleven modes of life that mostly belong
366 to suspension feeding lifestyles (Table 2). This is only two modes of life fewer than recorded
367 in the Werfen Formation, Italy (*sensu* Foster et al., 2017), owing to the absence of the epifaunal,
368 facultatively motile, attached, suspension feeding bivalve *Claraia* and scaphopods in this
369 study. The functional richness of samples ranges from 1 to 7 and functional effective diversity
370 ranges from 1 to 4.2 (Fig. 7E-H). Similar to the taxonomic results, the most functionally rich
371 samples are found in the Myophoria Beds Member, both in the shoal and mid-ramp
372 sedimentary facies (Fig. 7F). Trends in functional richness between the different members
373 follow those of species richness (Fig. 7A, 7E) and are also not significantly different between
374 members ($p=0.16$). Median functional richness increases from the inner- to mid-ramp
375 environment before a decline into the mid-ramp setting (Fig. 7F), but these differences are not
376 significant ($p=0.17$). The functional effective diversity of inner- and mid-ramp settings has
377 larger variances than the other sedimentary facies (Fig. 7H).

378

379 Changes in taxonomic composition

380 Cluster and SIMPROF analysis recognizes five larger groups (biofacies associations),
381 which are dominated by six taxa: *Austrotindaria*, *Coelostylina werfensis*, *Microconchus*,

382 *Natiria costata*, *Neoschizodus*, and cf. *Eumorphotis* (Table 3, Fig. 8). The SIMPER analysis of
383 these five biofacies associations shows that the samples within each group have an average
384 similarity of 45-78% (Table 3).



385

386 **FIGURE 8: Dendrogram of the compositions of the fossil assemblages of the samples from**
387 **the Servino Formation. A) Samples are clustered into five groups (1-5) based on taxonomic**
388 **composition; these are interpreted as different biofacies associations. B) Samples are clustered**
389 **into four groups (1-4) based on modes of life; these are interpreted as different ecofacies**
390 **associations. For biofacies and ecofacies descriptions, see Table 3.**

391

392 **TABLE 3: SIMPER analysis of biofacies (A) and ecofacies (B) associations.**
 393 Epi=epifaunal; Inf=shallow infaunal, Mot=slow-motile, FacU=factitively motile, unattached,
 394 StatA=stationary, attached, Susp=suspension feeder, Min=miner, Graz=grazer.
 395

A) Taxa	Contribution (%)	B) Modes of Life	Contribution (%)
Group 1	Average similarity: 45.5	Group 1	Average similarity: 67.5
<i>Austrotindaria</i>	90.3	Epi, Mot, Graz	85.9
Group 2	Average similarity: 68.58	Group 2	Average similarity: 59.7
<i>Natiria costata</i>	92.2	Inf, Mot, Min	84.7
Group 3	Average similarity: 53.21	Group 3	Average similarity: 74.0
<i>Microconchus</i>	100.0	Inf, FacU, Susp	77.2
Group 4	Average similarity: 77.9	Group 4	Average similarity: 66.3
<i>Coelostylinia werfensis</i>	94.6	Epi, StatA, Susp	89.0
Group 5	Average similarity: 52.6		
<i>Neoschizodus</i>	69.4		
<i>Coelostylinia werfensis</i>	82.7		

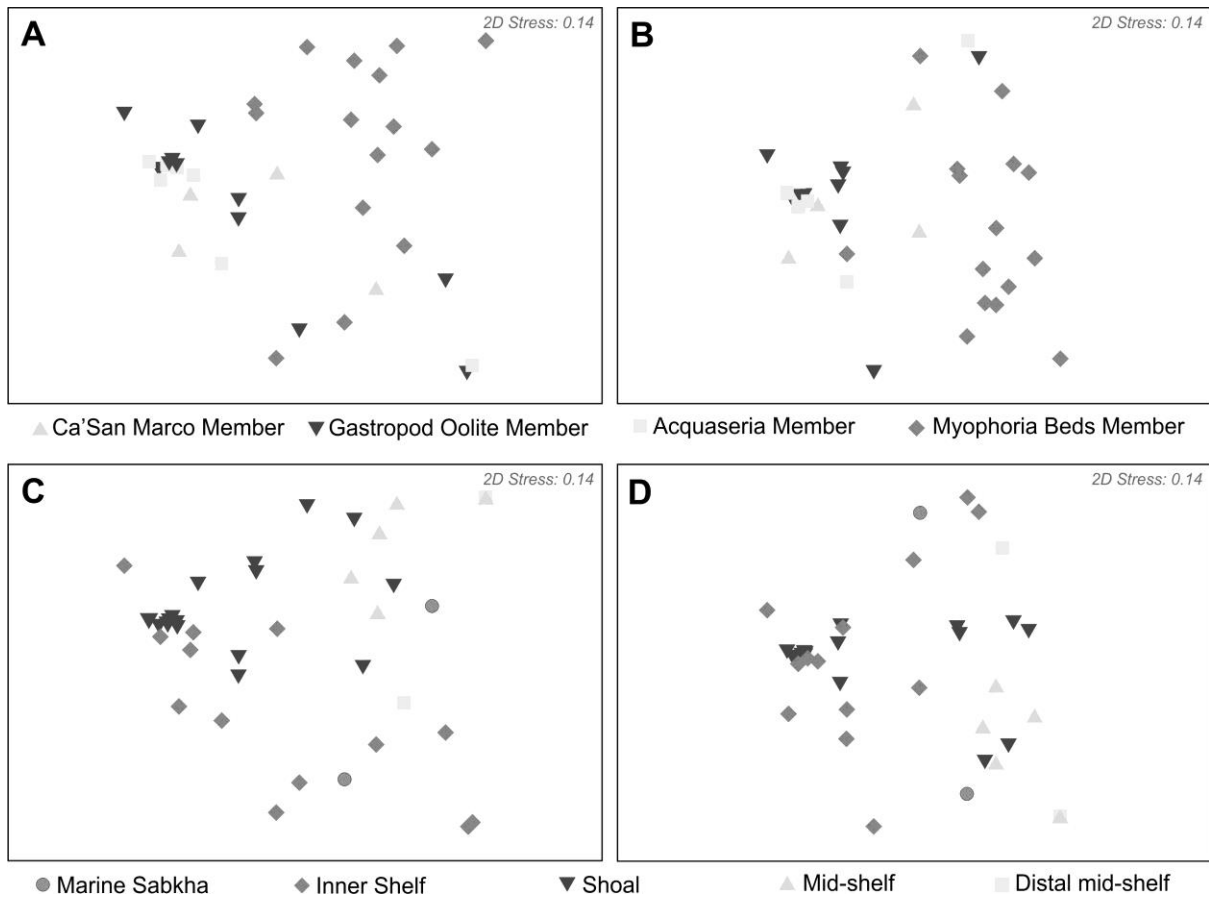
396

397

398 The *Coelostylinia werfensis* biofacies association is restricted to pre-Spathian strata
 399 (Group 4: Fig. 8A) and includes samples from inner ramp and shoal environments. The
 400 *Austrotindaria*, *Neoschizodus*, and *Microconchus* biofacies associations, however, occur in
 401 every substage (Fig. 8, Groups 1, 3 and 5). The samples from the pre-Spathian members are
 402 also distributed along an environmental gradient with inner ramp samples being dominated
 403 by both *Austrotindaria* and *Microconchus*, with only occasionally a high *C. werfensis*
 404 component, whereas the shoal environment is dominated mostly by *C. werfensis* (Fig. 8A).

405 The *Natiria costata* biofacies association is restricted to Spathian samples.

406 The nMDS plot (Fig. 9A) shows that the samples from the Myophoria Beds Member
 407 mostly plot as a separate group with a small overlap of the pre-Spathian samples. The cluster
 408 analysis (Fig. 8) and nMDS plots (Fig. 9) show that this is due to the *Neoschizodus* and *Natiria*
 409 *costata* associations being mostly restricted to the Myophoria Beds Member. The results of the
 410 PERMANOVA show that the compositions of samples from the Servino Formation members
 411 are significantly different from each other ($p < 0.01$). Pairwise comparisons, however, show that
 412 this is due to differences between the Spathian Myophoria Beds Member and pre-Spathian
 413 members (Table S1).



414

415 **FIGURE 9: Non-metric multi-dimensional scaling (nMDS) ordination of samples**
 416 **grouped according to the (A-B) members and (C-D) lithofacies of the Servino Formation.**
 417 **A,C) Ordination of samples according to their taxonomic composition. B,D) Ordination of**
 418 **samples according to their functional composition.**

419

420 The taxonomic composition of samples also differs between different environments:

421 the *N. costata* and *Austrotindaria* biofacies occurs in marine sabkha to outer ramp

422 environments; the *Neoschizodus* biofacies is restricted to the shoal; and the *Microconchus*

423 biofacies is restricted to the inner ramp environment (Fig. 9B). The PERMANOVA test

424 shows that the differences in taxonomic composition between the different sedimentary facies

425 are significant ($p < 0.001$), and the composition of samples from the inner ramp, shoal, and

426 mid-ramp are significantly different from one another (Table S2).

427

428
429
430
431
432
433
434
435
436
437
438
439
440
441
442
443
444
445
446
447
448
449
450
451

Changes in ecological composition

The SIMPER analysis shows only four ecofacies associations, each dominated by a different mode of life: 1) epifaunal, slow-moving grazers; 2) shallow-infaunal, slow-moving miners; 3) shallow-infaunal, facultatively motile, unattached, suspension feeders; and 4) epifaunal, facultatively motile, unattached, suspension feeders (Table 3; Supplementary material). At lower similarity levels these ecofacies associations can be recognized in the cluster analysis (Fig. 8B), and the SIMPER analysis shows that the samples within each group have an average similarity of 60-81% (Table 3), representing ecofacies associations.

Group 1 (Fig. 8B), dominated by epifaunal, slow-moving grazers, and Group 3, dominated by shallow-infaunal, facultatively motile, unattached, suspension feeders, are restricted to the Myophoria Beds Member. Group 4 (Fig. 8B) is dominated by epifaunal, facultatively motile, unattached, suspension feeders, and is restricted to the pre-Spathian Ca'San Marco, Gastropod Oolite, and Acquaseria Members. These two groups are not very similar to each other (Fig. 8B) and plot separately in the nMDS plot (Fig. 9C). The remaining ecofacies associations, on the other hand, occur in all of the sampled members and are not stratigraphically restricted (Fig. 9).

The nMDS plot (Fig. 9B) also shows that the pre-Spathian members plot separately to the Spathian samples with little overlap. The pairwise comparisons of the PERMANOVA test show that there is no significant difference in the position of the centroids of the Ca'San Marco, Gastropod Oolite, and Acquaseria Members (Fig. 9B; Table S3). The Spathian Myophoria Beds Member, however, does significantly differ from the pre-Spathian members (Table S3). When the samples are grouped according to their sedimentary facies there is no obvious trend in the distribution of samples (Fig. 9D).

452

Ichnology

453 Wrinkle marks and eight ichnotaxa were identified in this study. The Servino Formation
454 is characterized by low ichnogenic diversity, small burrows, and infrequent bioturbation.
455 Bioturbation is mostly limited to a few thin beds in the Servino Formation, except in the “Upper
456 Member” (Fig. 4). Ichnofabric indices of the Ca’San Marco Member, GOM, and Acquaseria
457 Member are low (ii1-2; Fig. 4). The Ca’San Marco Member has occurrences of *Diplocraterion*,
458 *Catenichnus*, *Skolithos*, *Arenicolites*, and *Planolites*, but these do not occur in sufficiently high
459 densities to disturb the primary sedimentary structures and burrow diameters in this member
460 are small (maximum = 9 mm, mean = 5 mm). In the Myophoria Beds Member, *Rhizocorallium*
461 *cf. irregulare*, *Laevicyclus*, *Palaeophycus*, *Skolithos*, and *Planolites* are found. Although
462 bioturbation is limited in this member, the ichnofabric indices and proportion of bioturbated
463 rock do increase upward (ii1-4; Fig. 4). Average burrow diameters in the Myophoria Beds
464 Member are small and comparable to the Ca’San Marco Member (average diameter 4 mm),
465 but they do record an increase in maximum size to 21 mm. The upper ~25 m of the “Upper
466 Member” records the onset of extensively bioturbated beds (ii3-5; Fig. 4) in shallow-subtidal
467 facies with *Rhizocorallium* and *Planolites*. Extensive bioturbation makes it difficult to identify
468 individual burrows but the sizes of those recognized are similar to the rest of the Servino
469 Formation (average 8 mm; max. 15 mm).

470

471

DISCUSSION

472 Unlike the Lower Triassic Werfen Formation, the Servino Formation has had relatively
473 little paleontological study (Cassinis, 1968; Gaetani, 1982; Neri, 1986; Posenato et al., 1996;
474 Twitchett, 1997, 2000; Sciunnach et al., 1999; Twitchett and Barras, 2004; Cassinis and Perotti,
475 2007). It is not as well exposed as the Werfen Formation, has fewer fossiliferous horizons
476 (Twitchett and Barras, 2004; Posenato, 2008b), and as a consequence, few taxa have previously

477 been recorded. The taxa identified (Table 2), the presence of *Coelostylinia werfensis*,
478 *Austrotindaria*, *Microconchus*, cf. *Eumorphotis*, *Neoschizodus*, and *Natiria costata* biofacies,
479 and the recorded ichnofauna, show that the Servino Formation has a similar faunal composition
480 to other Lower Triassic successions in Europe (cf. Fraiser et al., 2005; Twitchett and Oji 2005;
481 Foster et al. 2015; 2017; Pietsch et al., 2016; Petsios and Bottjer 2016; Broglio Loriga et al.
482 1990; Nützel and Schulbert 2005; Broglio Loriga and Posenato 1986; Broglio Loriga and Neri
483 1989; Neri and Posenato 1985; Posenato 1985; Broglio Loriga and Mirabella 1986). In
484 common with most Lower Triassic successions, the fauna of the Servino Formation are also
485 characterized as cosmopolitan opportunistic taxa that thrived in the aftermath of the late
486 Permian mass extinction (Schubert and Bottjer, 1995; Fraiser and Bottjer, 2004, 2007;
487 Kashiya and Oji, 2004; Shigeta et al., 2009; Fraiser, 2011; Hofmann et al., 2014; Pietsch et
488 al., 2014; Petsios and Bottjer, 2016). The difference in the overall diversity of the Servino
489 Formation compared to other study areas is, therefore, likely a sampling bias. The dominant
490 taxa that distinguish the different biofacies are, however, comparable to the Werfen Formation
491 and the differences in overall diversity are in the number of recorded rare taxa.

492

493 Persistent environmental stress delays recovery

494 The low diversity and dominant species of benthic assemblages in the Ca' San Marco
495 Member are similar to other pre-Spathian faunas recorded from the western Paleotethys (cf.
496 Nützel and Schulbert 2005; Foster et al. 2015, 2017; Hofmann et al. 2015; Pietsch et al. 2016).
497 In addition, the Ca' San Marco Member is characterized by shallow tier domichnia traces, an
498 absence of key taxa (e.g. crinoids) and ichnotaxa (e.g. *Thalassinoides*) that represent advanced
499 recovery, small body sizes, and low evenness, all of which together indicate an early stage of
500 recovery (Stage 2, *sensu* Twitchett, 2006). *Claraia aurita* and *C. intermedia* have been
501 identified in the Ca' San Marco Member in the Val Fontanalle and Valsassina localities,

502 respectively (Posenato et al., 1996; Cassinis, 1990). The assemblages of the Ca'San Marco
503 Member recorded at the locations in this study, however, notably lack *Claraia* and *Warthia*,
504 two taxa that are reported to have gone regionally extinct during the Dienerian in the western
505 Paleotethys (Posenato, 2008a; Hofmann et al., 2015; Foster et al., 2017a), which may suggest
506 diachronous deposition of the Servino Formation. The low diversity, lack of extensive
507 bioturbation, and small burrow sizes recorded in the Ca'San Marco Member are also
508 comparable to the Upper Siusi Member of the Werfen Formation (Twitchett and Barras, 2004),
509 which suggests that the units of the Ca'San Marco Member investigated in this study post-date
510 the late Griesbachian recovery pulse recognized in the Werfen Formation (Hofmann et al.,
511 2011; Foster et al., 2017) and the disappearance of *Claraia* and *Warthia*, i.e. post-date the
512 'Dienerian crisis' (Hofmann et al., 2015; Foster et al., 2017).

513 Benthic assemblages with compositions and recovery state similar to those recorded in
514 the Ca'San Marco Member are also recognized in the Gastropod Oolite and Acquaseria
515 Members (Fig. 9). The composition of the benthic faunas from the pre-Spathian Servino
516 Formation is also similar to other low latitude pre-Spathian faunas, e.g. Werfen Formation
517 (Fraiser et al., 2005; Nützel and Schulbert, 2005; Hofmann et al., 2015; Pietsch et al., 2016;
518 Foster et al., 2017a), Bódvaszilás Sandstone Formation (Foster et al., 2015), Sinbad Limestone
519 Formation (Fraiser et al., 2005; Nützel and Schulbert, 2005; Hofmann et al., 2014; Pietsch et
520 al., 2014), and the Dinwoody Formation (Hofmann et al., 2013).

521 The pre-Spathian faunas in the Servino Formation all occur above wave base and
522 seaward of the upper shoreface, i.e. within the hypothesized 'habitable zone' (Beatty et al.
523 2008), and do not record evidence of 'rapid recovery' (cf. Twitchett et al., 2004). The habitable
524 zone does not, therefore, guarantee immediate ecological recovery as had been previously
525 interpreted from other Lower Triassic sections. The oolitic limestones in the Gastropod Oolite
526 and Acquaseria Members are generally indicative of high energy and oxygenated environments

527 (Assereto and Rizzini, 1975), suggesting that a factor other than oxygen availability was
528 controlling the diversity and composition of benthic communities. The dominance of
529 microgastropods that resemble the modern euryhaline *Hydrobia* in the Gastropod Oolite
530 Member of the Werfen Formation led Nützel and Schulbert (2005) to suggest that brackish
531 conditions or strong salinity fluctuations caused stress to benthic communities at that time and
532 limited their recovery. Low diversity assemblages dominated by *Coelostylina werfensis* and
533 *Polygyrina* sp. show that microgastropods also dominated the Ca' San Marco, Gastropod Oolite,
534 and Acquaseria Members, which may suggest that salinity fluctuations were also limiting
535 recovery in the pre-Spathian Servino Formation. Geochemical and sedimentological proxies
536 for environmental conditions, such as eutrophication, are lacking for the Servino Formation
537 and make predicting local stressors equivocal. Other potential environmental stressors that
538 have been proposed as excluding or restricting benthic invertebrates elsewhere in shallow
539 marine environments during the Early Triassic, and may also have been a factor in the Servino
540 Formation, include high sediment fluxes (Algeo and Twitchett, 2010); eutrophication (Algeo
541 and Twitchett, 2010; Schobben et al., 2015); and high temperatures (Song et al., 2014).

542 An alternative hypothesis for the low diversity and slow recovery within the Early
543 Triassic is that the magnitude of the late Permian mass extinction was so catastrophic, a large
544 amount of time was required before pre-extinction levels of diversity could evolve (Erwin,
545 1998). This explanation has been used at the local-scale in an isolated platform setting in South
546 China, where an increase in taxonomic richness and evenness was recorded in the absence of
547 environmental change (Hautmann et al., 2015). The pace of recovery of taxonomic diversity in
548 the Servino Formation is, however, much lower and less ecologically complex than recorded
549 in other Early Triassic localities, e.g. Kesennuma, Japan (Kashiyama and Oji, 2004); Wadi
550 Wasit, Oman (Twitchett et al., 2004; Wheeley and Twitchett, 2005; Jacobsen et al., 2011; Oji
551 and Twitchett, 2015); central Svalbard (Foster et al. 2017b); and Guizhou, China (Hautmann

552 et al., 2011, 2015; Foster et al., 2018). Therefore, even though other explanations may explain
553 the slow apparent recovery and low diversity, persistent environmental stress from a number
554 of different possible stressors is interpreted as the main factor that limited the pace of recovery
555 through the pre-Spathian Servino Formation.

556

557 Two Pulses of Recovery in the Spathian

558 The Myophoria Beds Member was found to have the most taxonomically and
559 functionally rich samples in the Servino Formation (Fig. 7). The Myophoria Beds Member
560 records the first occurrences of *Holocrinus* sp. and *Rhizocorallium* cf. *irregulare*, which have
561 been used to indicate advanced recovery stages (Twitchett, 1999, 2006), and also record
562 increased bioturbation (ii1-4) and both a taxonomic and functional turnover (Figs. 8-9). This
563 recovery signal has also been recognized in other lower Spathian successions in central Europe
564 (Twitchett and Wignall, 1996; Twitchett, 1999; Twitchett and Barras, 2004; Posenato, 2008a;
565 Foster et al. 2015, 2017; Hofmann et al. 2015) and the western US (Schubert and Bottjer, 1995;
566 Fraiser, 2007; Fraiser and Bottjer, 2009; McGowan et al., 2009; Hofmann et al. 2013; 2014;
567 Pietsch et al. 2014; Petsios and Bottjer, 2016). This shift coincides globally with evidence for
568 a return to cooler seawater temperatures (Romano et al., 2012; Sun et al., 2012) and invigorated
569 ocean circulation (De Zanche and Farabegoli, 1981; Horacek et al. 2010).

570 This increase in diversity and the composition shift may, however, be a facies artefact,
571 as the mid-ramp facies is only sampled in the Myophoria Beds of the Servino Formation. The
572 mid-ramp Myophoria Beds facies are also similar to the mid-ramp facies of the Griesbachian
573 lower Siusi Member and the Spathian Val Badia Member in the nearby Werfen Formation,
574 Italy. The composition and ecological complexity of the Myophoria Beds Member fauna are
575 similar to the *N. costata* and *Neoschizodus* biofacies of the Val Badia Member, and completely
576 different from the lower Siusi Member biofacies (*sensu* Foster et al., 2017a), suggesting that

577 the Smithian/Spathian biofacies turnover and recovery signal is not a facies artefact, and most
578 likely a biological signal associated with more favorable environmental conditions for the
579 benthos. Even though the Myophoria Beds Member records relatively diverse communities
580 that are significantly different to their pre-Spathian counterparts, the fauna from distal mid-
581 ramp settings is restricted to thin tempestites which may suggest that the animals were
582 transported from shallower settings and did not normally inhabit the distal mid-ramp setting.
583 Furthermore, during fair-weather conditions the distal mid-ramp records low ichnofabric
584 indices (ii1) and an absence of ichnofauna (Fig. 4). Since trace fossils associated with the
585 burrowing activity of crustaceans (which are typically associated with well oxygenated
586 settings: Savrda, 2007) are found above wave base, the absence of bioturbation indicates that
587 conditions below wave base were likely to have been anoxic (Savrda, 2007), even into the
588 lower Spathian. Further work from proxies independent of the faunal records are, however,
589 required to confirm this observation.

590 In the upper part of the “Upper Member”, which tentatively correlates to the base of the
591 *Tirolites carniolicus* Zone, bioturbation increases from ii1 to ii5 within one meter of rock and
592 notably changes in the absence of a sedimentary facies change (Fig. 4). No shelly macrofossils
593 were recorded from this unit, so no comparative analyses of faunal composition or diversity
594 were possible. The strata of the “Upper Member” are exclusively composed of siltstones,
595 sandstones, and dolomitic sands, which reduces the preservation potential of calcitic shell
596 material due to early diagenetic dissolution (Hofmann et al., 2015). In addition, the “Upper
597 Member” is rarely well exposed, which adds another sampling bias. Thus, the absence of shelly
598 fossil assemblages in this unit is interpreted as a taphonomic effect. The Acquaseria Member
599 records the same lithologies and a similar facies to the “Upper Member” and even though the
600 clastic lithologies of the Acquaseria Member contain fossils preserved as molds, which are
601 absent in the “Upper Member”, the increased proportion of bioturbated sediment, and the

602 presence of *Rhizocorallium* suggests that the taphonomic bias does not explain an increase in
603 the recorded ecological complexity of marine communities. The extensive bioturbation and
604 presence of key ichnotaxa that are also recognized in other upper Spathian western
605 Paleotethyan localities, e.g. Aggtelek Karst (Hips, 1998; Foster et al., 2015), Balaton Highland
606 (Broglia Loriga et al., 1990), Bükk Mountains (Hips and Pelikán, 2002), and the Dolomites
607 (Twitchett and Wignall, 1996), suggests that the complexity of benthic ecosystems increased
608 in the upper Spathian. Evidence for increased complexity of benthic ecosystems in the upper
609 Spathian of western Paleotethys is recorded in a range of different depositional settings, i.e.
610 from peritidal to outer ramp/shelf settings. In the upper Spathian, animals are no longer
611 interpreted to have been restricted to the shallow subtidal environments as they expanded into
612 both coastal and deeper environments.

613 The proportion of bioturbated rock is also affected by changes in sedimentation rates
614 (Bentley et al., 2006), and the increased proportion of bioturbated rock in the “Upper Member”
615 could be due to a decline in sedimentation rates rather than a recovery signal. However, even
616 in western Paleotethyan locations where there are high linear sedimentation rates, there is an
617 increase in the proportion and extent of bioturbation (e.g. Szinpetri Limestone; Foster et al.,
618 2015). This recovery signal, therefore, appears to be a robust biological signal that coincides
619 globally with the formation of the oldest Mesozoic platform margin reefs (Great Bank of
620 Guizhou, China; Payne et al. 2006); *Placunopsis* bioherms (western US; Pruss et al. 2007); and
621 increased burrow sizes and ichnofabric indices in Anhui, China (Chen et al., 2011). The upper
622 Spathian, therefore, represents a recovery phase not previously recognized by semi-quantitative
623 recovery models (Twitchett et al., 2004; Twitchett 2006; Hofmann et al. 2014; Pietsch and
624 Bottjer 2014). In the “Upper Member” there is, however, a lack of shelly taxa, making it
625 impossible to compare the assemblages to the older Spathian strata. Based on a single sample
626 from the upper Spathian Szinpetri Limestone in the Aggtelek Karst, this upper Spathian

627 recovery, did not coincide with a significant biofacies change (Foster et al., 2015). Recognition
628 of this recovery phase in the field depends entirely on ichnofaunal records.

629

630

CONCLUSIONS

631 We have improved the stratigraphic framework of the Servino Formation with the
632 addition of new ammonoid and carbon isotope data and have undertaken the first quantitative
633 paleoecological analyses of the formation in order to document marine recovery after the late
634 Permian mass extinction. Benthic assemblages from the pre-Spathian members of the
635 formation are characterized by low taxonomic and functional diversities, low faunal
636 heterogeneity, low ichnodiversity, and lack key taxa indicative of ‘advanced recovery’, e.g.
637 crinoids. These assemblages were deposited in the hypothesized ‘habitable zone’ of wave-
638 aerated, nearshore ramp settings. Environmental stresses such as salinity fluctuations, high
639 turbidity, and/or eutrophication are likely to be the main causes for the absence of significant
640 recovery in the ‘habitable zone’ settings of the study sites in eastern Lombardy through the pre-
641 Spathian Early Triassic. The Spathian Myophoria Beds Member shows increased taxonomic
642 and functional diversity, the appearance of stenohaline taxa, the first appearance of key
643 ichnotaxa, and a significant shift in the composition of the benthos, all of which reflects an
644 advanced stage of recovery that has been recognized across western Paleotethys. These faunas
645 are also restricted to the proposed ‘habitable zone’. A late Spathian recovery pulse is recorded
646 in the uppermost Servino Formation, associated with increased bioturbation and expansion
647 beyond the wave-aerated ‘habitable zone’. This recovery pulse is also recognized in Italy,
648 Hungary, and China and correlates with the recovery of metazoan reef ecosystems in the
649 western US and China.

650

651

ACKNOWLEDGMENTS

652 Dario Sciunnach is thanked for helping with sampling permissions and discussions on the
653 Servino Formation. Louise Foster is thanked for her remote assistance during the fieldwork.
654 We would like to thank two anonymous reviewers and the associate editor who helped improve
655 the manuscript. A Natural Environment Research Council (NERC) grant (NE/I005641/2)
656 funded this study.

657

658

REFERENCES

- 659 ALGEO, T.J., CHEN, Z.Q., FRAISER, M.L., and TWITCHETT, R.J., 2011, Terrestrial–marine
660 teleconnections in the collapse and rebuilding of Early Triassic marine ecosystems:
661 Palaeogeography, Palaeoclimatology, Palaeoecology, v. 308, p. 1–11, doi:
662 10.1016/j.palaeo.2011.01.011.
- 663 ALGEO, T.J., and TWITCHETT, R.J., 2010, Anomalous Early Triassic sediment fluxes due to
664 elevated weathering rates and their biological consequences: *Geology*, v. 38, p. 1023–
665 1026, doi: 10.1130/G31203.1.
- 666 ALJINOVIĆ, D., KOLAR-JURKOVŠEK, T., and JURKOVŠEK, B., 2006, The Lower Triassic
667 shallow marine succession in Gorski Kotar Region (external Dinarides, Croatia):
668 Lithofacies and conodont dating: *Revista Italiana di Paleontologia e Stratigrafia*, v. 112,
669 p. 35–53.
- 670 ALJINOVIĆ, D., KOLAR-JURKOVŠEK, T., JURKOVŠEK, B., and HRVATOVIC, H., 2011, Conodont
671 dating of the Lower Triassic sedimentary rocks in the external Dinarides (Croatia and
672 Bosnia and Herzegovina): *Rivista Italiana di Paleontologia e Stratigrafia*, v. 117, p.
673 135–148.
- 674 ANDERSON, M.J., 2001, A new method for non parametric multivariate analysis of variance:
675 *Austral ecology*, v. 26, p. 32–46, doi: 10.1111/j.1442-9993.2001.01070.pp.x.
- 676 ANDERSON, M.J., and WALSH, D.C.I., 2013, PERMANOVA, ANOSIM, and the Mantel test
677 in the face of heterogeneous dispersions: What null hypothesis are you testing?
678 *Ecological Monographs*, v. 83, p. 557–574.
- 679 ASSERETO, R., BOSELLINI, A., SESTINI, N., and SWEET, W., 1973, The Permian-Triassic
680 boundary in the Southern Alps (Italy)., *in* 2. Canadian Society of Petroleum Geologists
681 Memoir: Calgary, Canada, p. 176–199.
- 682 ASSERETO, R., and RIZZINI, A., 1975, Reworked ferroan dolomite grains in the Triassic
683 “Oolite a Gasteropodi” of Camoniche Alps (Italy) as indicators of early diagenesis:
684 *Neues Jahrbuch für Geologie und Paläontologie*, v. 148, p. 215–232.
- 685 BAMBACH, R.K., BUSH, A.M., and ERWIN, D.H., 2007, Autecology and the filling of
686 Ecospace: Key Metazoan Radiations: *Palaeontology*, v. 50, p. 1–22.
- 687 BEATTY, T.W., ZONNEVELD, J.-P., and HENDERSON, C.M., 2008, Anomalously diverse Early
688 Triassic ichnofossil assemblages in northwest Pangea: A case for a shallow-marine
689 habitable zone: *Geology*, v. 36, p. 771–774.
- 690 BENTLEY, S., SHEREMET, A., and JAEGER, J., 2006, Event sedimentation, bioturbation, and

- 691 preserved sedimentary fabric: Field and model comparisons in three contrasting marine
692 settings: *Continental Shelf Research*, v. 26, p. 2108–2124.
- 693 BROGLIO LORIGA, C., GÓCZÁN, F., HAAS, J., LENNER, K., NERI, C., ORAVECZ-SCHEFFER, A.,
694 POSENATO, R., SZABO, I., and TÓTH-MAKK, A., 1990, The Lower Triassic sequence of
695 the Dolomites (Italy) and Transdanubian mid-mountains (Hungary) and their
696 correlation: *Memorie di Scienze Geologiche*, Padova, v. 42, p. 41–103.
- 697 BROGLIO LORIGA, C., and MIRABELLA, S., 1986, Il genere *Eumorphotis* Bittner, 1901 nella
698 biostratigrafia dello Scitico, formazione di Werfen (Dolomiti): *Memorie di Scienze*
699 *Geologiche*, v. 38, p. 245–281.
- 700 BROGLIO LORIGA, C., and NERI, C., 1989, *Spirorbis* valvata community from Werfen
701 Formation: an example of the Scythian oligotypy (Lower Scythian, Southern Alps,
702 Italy): *Atti 3 Simposio di Ecologia e Paleoecologia delle Comunità bentoniche*,
703 *Università di Catania*, Catania, p. 123–140.
- 704 BROGLIO LORIGA, C., and POSENATO, R., 1986, *Costatoria* (*Costatoria?*) *subrotunda* (Bittner,
705 1901), a Smithian (Lower Triassic) marker from Tethys.: *Rivista Italiana di*
706 *Paleontologia e Stratigrafia*, v. 92, p. 189–200.
- 707 BURGESS, S.D., and BOWRING, S., 2015, High-precision geochronology confirms voluminous
708 magmatism before, during, and after Earth's most severe extinction: *Science Advances*,
709 v. 1, p. e1500470.
- 710 CASSINIS, G., 1990, Itinerario n° 3 – Val Trompia, *in* Bianca, M., Gelati, R., and Gregnanin,
711 A., eds., *Alpi E Prealpi Lombarde*, *Guide Geologiche Regionali*: Milano, p. 291.
- 712 CASSINIS, G., 1968, Studio stratigrafico del “Servino” di Passo Valdì (Trias inferiore
713 dell’Alta Val Caffaro): *Atti dell’Istituto di Geologia dell’Università Pavia*, v. 19, p. 15–
714 39.
- 715 CASSINIS, G., DURAND, M., and RONCHI, A., 2007, Remarks on the Permian-Triassic
716 transition in Central and Eastern Lombardy (Southern Alps, Italy) *Apuntes sobre el*
717 *tránsito Pérmico-Triásico en Lombardía central y oriental (Alpes Meridionales, Italia)*:
718 *Journal of Iberian Geology*, v. 33, p. 143–162.
- 719 CASSINIS, G., and PEROTTI, C.R., 2007, A stratigraphic and tectonic review of the Italian
720 Southern Alpine Permian: *Palaeoworld*, v. 16, p. 140–172, doi:
721 10.1016/j.palwor.2007.05.004.
- 722 CHEN, Z.-Q., FRAISER, M.L., and BOLTON, C., 2012, Early Triassic trace fossils from
723 Gondwana Interior Sea: Implication for ecosystem recovery following the end-Permian
724 mass extinction in south high-latitude region: *Gondwana Research*, v. 22, p. 238–255,
725 doi: 10.1016/j.gr.2011.08.015.
- 726 CHEN, Y., KOLAR-JURKOVŠEK, T., JURKOVŠEK, B., ALJINOVIĆ, D., and RICHOSZ, S., 2016,
727 Early Triassic conodonts and carbonate carbon isotope record of the Idrija-Žiri area,
728 Slovenia: *Palaeogeography, Palaeoclimatology, Palaeoecology*, v. 444, p. 84–100, doi:
729 10.1016/j.palaeo.2015.12.013.
- 730 CHEN, Z.-Q., TONG, J., and FRAISER, M.L., 2011, Trace fossil evidence for restoration of
731 marine ecosystems following the end-Permian mass extinction in the Lower Yangtze
732 region, South China: *Palaeogeography, Palaeoclimatology, Palaeoecology*, v. 299, p.
733 449–474, doi: 10.1016/j.palaeo.2010.11.023.
- 734 CHEN, Z.-Q., TONG, J., KAIHO, K., and KAWAHATA, H., 2007, Onset of biotic and

- 735 environmental recovery from the end-Permian mass extinction within 1-2 million years:
736 A case study of the Lower Triassic of the Meishan section, South China:
737 *Palaeogeography Palaeoclimatology Palaeoecology*, v. 252, p. 176–187.
- 738 CLARKE, K.R., and WARWICK, 2001, *Change In Marine Communities: An Approach To*
739 *Statistical Analysis And Interpretation (2nd Edition): PRIMER-E, Plymouth.*
- 740 DOGLIONI, C., 1987, Tectonics of the Dolomites (southern alps, northern Italy): *Journal of*
741 *Structural Geology*, v. 9, p. 181–193, doi: 10.1016/0191-8141(87)90024-1.
- 742 DE DONATIS, S., and FALLETTI, P., 1999, The Early Triassic Servino Formation of the Monte
743 Guglielmo area and relationships with the Servino of Trompia and Camonica Valleys
744 (Brescian Prealps, Lombardy): *Memorie di Scienze Geologiche*, v. 51, p. 91–101.
- 745 DROSER, M.L., and BOTTJER, D.J., 1993, Trends and patterns of Phanerozoic ichnofabrics:
746 *Annual Review of Earth and Planetary Sciences*, v. 21, p. 205–225.
- 747 ERWIN, D.H., 1998, The end and the beginning: recoveries from mass extinctions: *TREE*, v.
748 13, p. 344–349.
- 749 ERWIN, D.H., and Pan, H-Z., 1996, Permo-Triassic mass extinction recoveries and radiations:
750 gastropods after the Permo-Triassic mass extinction: *Geol. Soc. Lond. Spec. Publ.* v.
751 102, p. 223–229. <http://dx.doi.org/10.1144/GSL.SP.1996.001.01.15>.
- 752 FOSTER, W.J., DANISE, S., PRICE, G.D., and TWITCHETT, R.J., 2017a, Subsequent biotic crises
753 delayed marine recovery following the late Permian mass extinction event in northern
754 Italy: *PLoS ONE*, v. 12, p. e0172321.
- 755 FOSTER, W.J., DANISE, S., SEDLACEK, A., PRICE, G.D., HIPS, K., and TWITCHETT, R.J., 2015,
756 Environmental controls on the post-Permian recovery of benthic, tropical marine
757 ecosystems in western Palaeotethys (Aggtelek Karst, Hungary): *Palaeogeography,*
758 *Palaeoclimatology, Palaeoecology*, v. 440, p. 374–394, doi:
759 10.1016/j.palaeo.2015.09.004.
- 760 FOSTER, W.J., DANISE, S., and TWITCHETT, R.J., 2017b, A silicified Early Triassic marine
761 assemblage from Svalbard: *Journal of Systematic Palaeontology*, v. 15, p. 851–877, doi:
762 10.1080/14772019.2016.1245680.
- 763 FOSTER, W.J., LEHRMANN, D.J., YU, M.Y., JI, L., and MARTINDALE, R.C., 2018,
764 Persistent environmental stress delayed the recovery of marine communities in the
765 aftermath of the latest Permian mass extinction: *Paleoceanography and*
766 *Paleoclimatology*, Doi:10.1002/2018PA003328
- 767 FOSTER, W.J., and TWITCHETT, R.J., 2014, Functional diversity of marine ecosystems after
768 the Late Permian mass extinction event: *Nature Geoscience*, v. 7, p. 233–238, doi:
769 10.1038/NGEO2079.
- 770 FOSTER, W.J., and SEBE, K., 2017, Recovery and diversification of marine communities
771 following the late Permian mass extinction event in the western Palaeotethys: *Global*
772 *and Planetary Change*, v. 155, p. 165–177.
- 773 FRAISER, M.L., 2011, Paleoeecology of secondary tierers from Western Pangean tropical
774 marine environments during the aftermath of the end-Permian mass extinction:
775 *Palaeogeography, Palaeoclimatology, Palaeoecology*, v. 308, p. 181–189, doi:
776 10.1016/j.palaeo.2010.12.002.
- 777 FRAISER, M.L., and BOTTJER, D.J., 2004, The Non-Actualistic Early Triassic Gastropod
778 Fauna: A Case Study of the Lower Triassic Sinbad Limestone Member: *PALAIOS*, v.

- 779 19, p. 259–275.
- 780 FRAISER, M.L., and BOTTJER, D.J., 2007, When bivalves took over the world: Paleobiology,
781 v. 33, p. 397–413.
- 782 FRAISER, M.L., TWITCHETT, R.J., and BOTTJER, D.J., 2005, Unique microgastropod biofacies
783 in the Early Triassic: Indicator of long-term biotic stress and the pattern of biotic
784 recovery after the end-Permian mass extinction: *C. R. Palevol*, v. 4, p. 543–552, doi:
785 10.1016/j.crpv.2005.04.006.
- 786 GAETANI, M., 1982, Elementi stratigrafici e strutturali della galleria Bellano-Varenna (Nuova
787 S.S. 36) (Como): *Rivista Italiana di Paleontologia e Stratigrafia*, v. 88, p. 1–10.
- 788 GRASBY, S.E., BEAUCHAMP, B., EMBRY, A., and SANEI, H., 2013, Recurrent Early Triassic
789 ocean anoxia: *Geology*, v. 41, p. 175–178, doi: 10.1130/G33599.1.
- 790 GRICE, K., CHANGQUN, C., LOVE, G., BOTTCHER, M., TWITCHETT, R., GROSJEAN, E.,
791 SUMMONS, R., TURGEON, S., DUNNING, W., and JIN, Y., 2005, Photic Zone Euxinia
792 During the Permian-Triassic Superanoxic Event: *Science*, v. 307, p. 706–709.
- 793 HAUTMANN, M., BAGHERPOUR, B., BROSE, M., FRISK, Å., HOFMANN, R., BAUD, A.,
794 NÜTZEL, A., GOUEMAND, N., and BUCHER, H., 2015, Competition in slow motion: the
795 unusual case of benthic marine communities in the wake of the end-Permian mass
796 extinction: *Palaeontology*, v. 58, p. 871–901, doi: 10.1111/pala.12186.
- 797 HAUTMANN, M., BUCHER, H., BRÜHWILER, T., GOUEMAND, N., KAIM, A., and NÜTZEL, A.,
798 2011, An unusually diverse mollusc fauna from the earliest Triassic of South China and
799 its implications for benthic recovery after the end-Permian biotic crisis: *Geobios*, v. 44,
800 p. 71–85, doi: 10.1016/j.geobios.2010.07.004.
- 801 HE, W.-H., SHI, G.R., TWITCHETT, R.J., ZHANG, Y., ZHANG, K.-X., SONG, H.-J., YUE, M.-L.,
802 WU, S.-B., WU, H.-T., YANG, T.-L., and XIAO, Y.-F., 2015, Late Permian marine
803 ecosystem collapse began in deeper waters: evidence from brachiopod diversity and
804 body size changes: *Geobiology*, v. 13, p. 123–138, doi: 10.1111/gbi.12119.
- 805 HIPS, K., 1998, Lower Triassic storm-dominated ramp sequence in northern Hungary: an
806 example of evolution from homoclinal through distally steepened ramp to Middle
807 Triassic flat-topped platform: *Geological Society, London, Special Publications*, v. 149,
808 p. 315–338, doi: 10.1144/GSL.SP.1999.149.01.15.
- 809 HIPS, K., and PELIKÁN, P., 2002, Lower Triassic shallow marine succession in the Bukk
810 Mountains, NE Hungary: *Geologica Carpathica*, v. 53, p. 351–367.
- 811 HOFMANN, R., HAUTMANN, M., BRAYARD, A., NÜTZEL, A., BYLUND, K.G., JENKS, J.F.,
812 VENNIN, E., OLIVIER, N., and BUCHER, H., 2014, Recovery of benthic marine
813 communities from the end-Permian mass extinction at the low latitudes of eastern
814 Panthalassa: *Palaeontology*, v. 57, p. 547–589, doi: 10.1111/pala.12076.
- 815 HOFMANN, R., HAUTMANN, M., and BUCHER, H., 2013, A New Paleoeological Look at the
816 Dinwoody Formation (Lower Triassic, Western USA): Intrinsic Versus Extrinsic
817 Controls on Ecosystem Recovery After the End-Permian Mass Extinction: *Journal of*
818 *Paleontology*, v. 87, p. 854–880, doi: 10.1666/12-153.
- 819 HOFMANN, R., HAUTMANN, M., and BUCHER, H., 2015, Recovery dynamics of benthic
820 marine communities from the Lower Triassic Werfen Formation, northern Italy: *Lethaia*,
821 v. 48, p. 474–496, doi: 10.1111/let.12121.
- 822 HORACEK, M., BRANDNER, R., and ABART, R., 2007, Carbon isotope record of the P/T

- 823 boundary and the Lower Triassic in the Southern Alps: Evidence for rapid changes in
824 storage of organic carbon: *Palaeogeography, Palaeoclimatology, Palaeoecology*, v. 252,
825 p. 347–354, doi: 10.1016/j.palaeo.2006.11.049.
- 826 HORACEK, M., BRANDNER, R., RICHOSZ, S., and POVODEN-KARADENIZ, E., 2010, Lower
827 Triassic sulphur isotope curve of marine sulphates from the Dolomites, N-Italy:
828 *Palaeogeography, Palaeoclimatology, Palaeoecology*, v. 290, p. 65–70, doi:
829 10.1016/j.palaeo.2010.02.016.
- 830 HORACEK, M., KOIKE, T., and RICHOSZ, S., 2009, Lower Triassic $\delta^{13}\text{C}$ isotope curve from
831 shallow-marine carbonates in Japan, Panthalassa realm: Confirmation of the Tethys
832 $\delta^{13}\text{C}$ curve: *Journal of Asian Earth Sciences*, v. 36, p. 481–490, doi:
833 10.1016/j.jseaes.2008.05.005.
- 834 JACOBSEN, N.D., TWITCHETT, R.J., and KRISTYN, L., 2011, Palaeoecological methods for
835 assessing marine ecosystem recovery following the Late Permian mass extinction event:
836 *Palaeogeography, Palaeoclimatology, Palaeoecology*, v. 308, p. 200–212, doi:
837 10.1016/j.palaeo.2010.04.024.
- 838 JOST, L., 2007, Partitioning diversity into independent alpha and beta components: *Ecology*,
839 v. 88, p. 2427–2439, doi: 10.1890/06-1736.1.
- 840 KASHIYAMA, Y., and OJI, T., 2004, Low-diversity shallow marine benthic fauna from the
841 Smithian of northeast Japan: paleoecologic and paleobiogeographic implications:
842 *Paleontological Research*, v. 8, p. 199–218, doi: 10.2517/prpsj.8.199.
- 843 KEARSEY, T., TWITCHETT, R.J., PRICE, G.D., and GRIMES, S.T., 2009, Isotope excursions and
844 palaeotemperature estimates from the Permian/Triassic boundary in the Southern Alps
845 (Italy): *Palaeogeography, Palaeoclimatology, Palaeoecology*, v. 279, p. 29–40, doi:
846 10.1016/j.palaeo.2009.04.015.
- 847 KNOLL, A.H., BAMBACH, R.K., PAYNE, J.L., PRUSS, S., and FISCHER, W.W., 2007,
848 Paleophysiology and end-Permian mass extinction: *Earth and Planetary Science Letters*,
849 v. 256, p. 295–313, doi: 10.1016/j.epsl.2007.02.018.
- 850 MCGHEE, G.R., SHEEHAN, P.M., BOTTJER, D.J., and DROSER, M.L., 2004, Ecological ranking
851 of Phanerozoic biodiversity crises: Ecological and taxonomic severities are decoupled:
852 *Palaeogeography, Palaeoclimatology, Palaeoecology*, v. 211, p. 289–297, doi:
853 10.1016/j.palaeo.2004.05.010.
- 854 MCGOWAN, A.J., SMITH, A.B., TAYLOR, P.D., 2009, Faunal diversity, heterogeneity and
855 body size in the Early Triassic: testing post-extinction paradigms in the Virgin
856 Limestone of Utah, USA: *Aust. J. Earth Sci.* v. 56, p. 859–872. doi:
857 10.1080/08120090903002839. NABBefeld, B., GRICE, K., TWITCHETT, R.J., SUMMONS,
858 R.E., HAYS, L., BÖTTCHER, M.E., and ASIF, M., 2010, An integrated biomarker, isotopic
859 and palaeoenvironmental study through the Late Permian event at Lusitaniadalen,
860 Spitsbergen: *Earth and Planetary Science Letters*, v. 291, p. 84–96, doi:
861 10.1016/j.epsl.2009.12.053.
- 862 NERI, C., 1986, Servino (Werfen Formation). Some lithostratigraphical remarks. Maniva-
863 Croce Domini road, around the small glacial circle to SSW-W of M.Rondenino. Height
864 2000m, *in* Field Guide-Book, Field Conference on Permian and Permian-Triassic
865 Boundary in the South-Alpine Segment of the Western Tethys: p. 163–166.
- 866 NERI, C., and POSENATO, R., 1985, New biostratigraphical data on uppermost Werfen
867 Formation of western Dolomites (Trento, Italy): *Geologisch– Paläontologische*

- 868 Mitteilungen Innsbruck, v. 14, p. 83–107.
- 869 NOVACK-GOTTSHALL, P.M., 2007, Using a theoretical ecospace to quantify the ecological
870 diversity of paleozoic and modern marine biotas: *Paleobiology*, v. 33, p. 273–294.
- 871 NÜTZEL, A., and SCHULBERT, C., 2005, Facies of two important Early Triassic gastropod
872 lagerstätten: implications for diversity patterns in the aftermath of the end-Permian mass
873 extinction: *Facies*, v. 51, p. 480–500, doi: 10.1007/s10347-005-0074-5.
- 874 OJI, T., and TWITCHETT, R.J., 2015, The oldest post-Palaeozoic crinoid and Permian-Triassic
875 origins of the articulata (echinodermata): *Zoological science*, v. 32, p. 211–5, doi:
876 10.2108/zs140240.
- 877 PAYNE, J.L., LEHRMANN, D.J., CHRISTENSEN, S., WEI, J., and KNOLL, A.H., 2006a,
878 Environmental and Biological Controls on the Initiation and Growth of a Middle
879 Triassic (Anisian) Reef Complex on the Great Bank of Guizhou , Guizhou Province ,
880 China: p. 325–343, doi: 10.2110/palo.2005.P05-58e.
- 881 PAYNE, J.L., LEHRMANN, D.J., WEI, J., and KNOLL, A.H., 2006b, The Pattern and Timing of
882 Biotic Recovery from the End-Permian Extinction on the Great Bank of Guizhou,
883 Guizhou Province, China: *Palaios*, v. 21, p. 63–85.
- 884 PAYNE, J.L., LEHRMANN, D.J., WEI, J., ORCHARD, M.J., SCHRAG, D.P., and KNOLL, A.H.,
885 2004, Large perturbations of the carbon cycle during recovery from the end-permian
886 extinction.: *Science (New York, N.Y.)*, v. 305, p. 506–509, doi:
887 10.1126/science.1097023.PAYNE, J.L., SUMMERS, M., REGO, B.L., ALTINER, D.,
888 WEI, J.Y., YU, M.Y., LEHRMANN, D.J., 2011, Early and Middle Triassic trends in
889 diversity, evenness, and size of foraminifers on a carbonate platform in south China:
890 implications for tempo and mode of biotic recovery from the end-Permian mass
891 extinction: *Paleobiology* v. 37, p. 409–425. doi: 10.1666/08082.1.
- 892 PETSIOS, E., and BOTTJER, D.J., 2016, Quantitative analysis of the ecological dominance of
893 benthic disaster taxa in the aftermath of the end-Permian mass extinction: *Paleobiology*,
894 v. 42, p. 380–393, doi: 10.1017/pab.2015.47.
- 895 PIETSCH, C., and BOTTJER, D.J., 2014, The importance of oxygen for the disparate recovery
896 patterns of the benthic macrofauna in the Early Triassic: *Earth-Science Reviews*, v. 137,
897 p. 65–84, doi: 10.1016/j.earscirev.2013.12.002.
- 898 PIETSCH, C., MATA, S.A., and BOTTJER, D.J., 2014, High temperature and low oxygen
899 perturbations drive contrasting benthic recovery dynamics following the end-Permian
900 mass extinction: *Palaeogeography, Palaeoclimatology, Palaeoecology*, v. 399, p. 98–
901 113, doi: 10.1016/j.palaeo.2014.02.011.
- 902 PIETSCH, C., PETSIOS, E., and BOTTJER, D.J., 2016, Sudden and extreme hyperthermals, low-
903 oxygen, and sediment influx drove community phase shifts following the end-Permian
904 mass extinction: *Palaeogeography, Palaeoclimatology, Palaeoecology*, v. 451, p. 183–
905 196, doi: 10.1016/j.palaeo.2016.02.056.
- 906 POSENATO, R., 2008a, Global correlations of mid Early Triassic events: The
907 Induan/Olenekian boundary in the Dolomites (Italy): *Earth-Science Reviews*, v. 91, p.
908 93–105, doi: 10.1016/j.earscirev.2008.09.001.
- 909 POSENATO, R., 2008b, Patterns of bivalve biodiversity from Early to Middle Triassic in the
910 Southern Alps (Italy): Regional vs. global events: *Palaeogeography, Palaeoclimatology,*
911 *Palaeoecology*, v. 261, p. 145–159, doi: DOI 10.1016/j.palaeo.2008.01.006.

- 912 POSENATO, R., 1992, Tirolites (Ammonoidea) from the Dolomites, Bakony and Dalmatia:
913 Taxonomy and biostratigraphy: *Eclogae Geologicae Helvetiae*, v. 85, p. 893–929, doi:
914 10.5169/seals-167062.
- 915 POSENATO, R., 1985, Un'Associazione oligotipica a *Neoschizodus ovatus* (GOLDFUSS)
916 della formazione di Werfen (Triassico inf-Dolomiti): *Atti 3 Simposio di Ecologia e*
917 *Paleoecologia delle Comunità bentoniche*, p. 141–153.
- 918 POSENATO, R., SCIUNNACH, D., and GARZANTI, E., 1996, First report of *Claraia* (bivalvia) in
919 the Servino formation (Lower Triassic) of the western Orobian Alps, Italy: *Rivista Italiana*
920 *di Paleontologia e Stratigrafia*, v. 102, p. 201–210.
- 921 PRUSS, S.B., PAYNE, J.L., and BOTTJER, D.J., 2007, Placunopsis Bioherms: the First
922 Metazoan Buildups Following the End-Permian Mass Extinction: *Palaios*, v. 22, p. 17–
923 23, doi: 10.2110/palo.2005.p05-050r.
- 924 ROMANO, C., GOUEMAND, N., VENNEMANN, T.W., WARE, D., SCHNEEBELI-HERMANN, E.,
925 HOCHULI, P. a., BRÜHWILER, T., BRINKMANN, W., and BUCHER, H., 2012, Climatic and
926 biotic upheavals following the end-Permian mass extinction: *Nature Geoscience*, v. 6, p.
927 57–60, doi: 10.1038/ngeo1667.
- 928 SCHOBEN, M., STEBBINS, A., GHADERI, A., STRAUSS, H., KORN, D., and KORTE, C., 2015,
929 Flourishing ocean drives the end-Permian marine mass extinction: *Proceedings of the*
930 *National Academy of Sciences*, v. 112, p. 10298–10303, doi: 10.1073/pnas.1503755112.
- 931 SCHUBERT, J.K., and BOTTJER, D.J., 1995, Aftermath of the Permian-Triassic mass extinction
932 event: Paleocology of Lower Triassic carbonates in the western USA:
933 *Palaeogeography, Palaeoclimatology, Palaeoecology*, v. 116, p. 1–39, doi:
934 10.1016/0031-0182(94)00093-N.
- 935 SCIUNNACH, D., GARZANTI, E., POSENATO, R., and RODEGHIERO, F., 1999, Stratigraphy of
936 the Servino Formation (Lombardy, Southern Alps): towards a refined correlation with
937 the Werfen Formation of the Dolomites: *Memorie di Scienze Geologiche*, v. 51, p. 103–
938 118.
- 939 SHIGETA, Y., ZAKHAROV, Y.D., MAEDA, H., and POPOV, A.M., 2009, The lower Triassic
940 system in the Abrek Bay area, South Primorye, Russia: *National Museum of Nature and*
941 *Science Monographs No.38*, Tokyo.
- 942 SUN, Y., JOACHIMSKI, M.M., WIGNALL, P.B., YAN, C., CHEN, Y., JIANG, H., WANG, L., and
943 LAI, X., 2012, Lethally Hot Temperatures During the Early Triassic Greenhouse:
944 *Science*, v. 338, p. 366–370, doi: 10.1126/science.1224126.
- 945 SAVRDA, C.E., 2007, Trace fossils and marine benthic oxygenation. In: MILLER, W.,
946 (EDITOR), *Trace Fossils* p. 149-158.
- 947 SWEET, W., MOSHER, L., CLARK, D., COLLINSON, J., and HASENMUELLER, W., 1971,
948 Conodont biostratigraphy of the Triassic, in *Symposium on Conodont Biostratigraphy*.
949 *Geological Society of America Memoirs 127*: p. 499.
- 950 TÖRÖK, A., 1998, Controls on development of Mid-Triassic ramps: examples from southern
951 Hungary, in *Carbonate Ramps*: Geological Society, London, Special Publications, 149,
952 p. 339–367.
- 953 TWITCHETT, R., 2000, A high resolution biostratigraphy for the Lower Triassic of northern
954 Italy: *Palaeontol. Assoc. Newslett*, v. 43, p. 19–22.
- 955 TWITCHETT, R.J., 1997, No Title: University of Leeds.

- 956 TWITCHETT, R.J., 1999, Palaeoenvironments and faunal recovery after the end-Permian mass
957 extinction: *Palaeogeography, Palaeoclimatology, Palaeoecology*, v. 154, p. 27–37, doi:
958 10.1016/S0031-0182(99)00085-1.
- 959 TWITCHETT, R.J., 2006, The palaeoclimatology, palaeoecology and palaeoenvironmental
960 analysis of mass extinction events: *Palaeogeography, Palaeoclimatology, Palaeoecology*,
961 v. 232, p. 190–213, doi: 10.1016/j.palaeo.2005.05.019.
- 962 TWITCHETT, R.J., and BARRAS, C.G., 2004, Trace fossils in the aftermath of mass extinction
963 events: Geological Society, London, Special Publications, v. 228, p. 397–418, doi:
964 10.1144/GSL.SP.2004.228.01.18.
- 965 TWITCHETT, R.J., KRYSSTYN, L., BAUD, A., WHEELLEY, J.R., and RICHOZ, S., 2004, Rapid
966 marine recovery after the end-Permian mass-extinction event in the absence of marine
967 anoxia: *Geology*, v. 32, p. 805, doi: 10.1130/G20585.1.
- 968 TWITCHETT, R.J., and OJI, T., 2005, Early Triassic recovery of echinoderms: *Comptes*
969 *Rendus Palevol*, v. 4, p. 531–542, doi: 10.1016/j.crpv.2005.02.006.
- 970 TWITCHETT, R.J., and WIGNALL, P.B., 1996, Trace fossils and the aftermath of the Permo-
971 Triassic mass extinction: evidence from northern Italy: *Palaeogeography*,
972 *Palaeoclimatology, Palaeoecology*, v. 124, p. 137–151, doi: 10.1016/0031-
973 0182(96)00008-9.
- 974 WHEELLEY, J.R., and TWITCHETT, R.J., 2005, Palaeoecological significance of a new
975 Griesbachian (Early Triassic) gastropod assemblage from Oman: *Lethaia*, v. 38, p. 37–
976 45, doi: 10.1080/0024116051003150.
- 977 WIGNALL, P.B., BOND, D.P.G., SUN, Y., GRASBY, S.E., BEAUCHAMP, B., JOACHIMSKI, M.M.,
978 and BLOMEIER, D.P.G., 2016, Ultra-shallow-marine anoxia in an Early Triassic shallow-
979 marine clastic ramp (Spitsbergen) and the suppression of benthic radiation: *Geological*
980 *Magazine*, v. 153, p. 316–331, doi: 10.1017/S0016756815000588.
- 981 WIGNALL, P.B., and TWITCHETT, R.J., 1996, Oceanic Anoxia and the End Permian Mass
982 Extinction: *Science*, v. 272, p. 1155–1158, doi: 10.1126/science.272.5265.1155.
- 983 ZHANG, L., ZHAO, L., CHEN, Z.-Q., ALGEO, T.J., LI, Y., and CAO, L., 2015, Amelioration of
984 marine environments at the Smithian–Spathian boundary, Early Triassic:
985 *Biogeosciences*, v. 12, p. 1597–1613, doi: 10.5194/bg-12-1597-2015.
- 986 ZHANG, Y., SHI, G. R., WU, H. T., YANG, T. L., HE, W. H., YUAN, A. H., and LEI, Y.
987 2017, Community replacement, ecological shift and early warning signals prior to the
988 end-Permian mass extinction: A case study from a nearshore clastic-shelf section in
989 South China: *Palaeogeography, Palaeoclimatology, Palaeoecology*, v. 487, p. 118-
990 135. ZONNEVELD, J., GINGRAS, M.K., and BEATTY, T.W., 2010, Diverse Ichnofossil
991 Assemblages Following the P-T Mass Extinction, Lower Triassic, Alberta and British
992 Columbia, Canada: Evidence for Shallow Marine Refugia on the Northwestern Coast of
993 Pangaea: *Palaios*, v. 25, p. 368–392, doi: 10.2110/palo.2009.p09-135r.